THE UNIVERSITY of EDINBURGH

Edinburgh Research Explorer

A role for macrophages in hematopoiesis in the embryonic head

OPEN ACCESS

A role for macrophages in hematopoiesis in the embryonic head

Zhuan Li[1,2*], Samanta A. Mariani[1], Carmen Rodriguez-Seoane[1], Wenyan He[3], Xiaowei Ning[4], Bing Liu[4], Chris S. Vink[1], and Elaine Dzierzak[1*]

[1]The University of Edinburgh, Centre for Inflammation Research, UK; [2]Southern Medical University, School of Basic Medical Sciences, Department of Developmental Biology, Guangzhou, China; [3]China National Clinical Research Center for Neurological Diseases, Beijing Tiantan Hospital, Capital Medical University, Beijing, China; and [4]Laboratory of Oncology, Fifth Medical Center, General Hospital of PLA, Beijing, China.

Running title: Macrophages affect head hematopoietic development

Abstract: 193 words
Text: 4,131 words
Figures: 7
Supplementary material: 4 figures, 6 tables

Key words: macrophage; hematopoietic development; embryo, MacGreen; Cx3cr1; Csf1r; head; EHT; OP9-DL1

*Co-Corresponding authors:

Elaine Dzierzak
University of Edinburgh
Centre for Inflammation Research
Queens Medical Research Institute
47 Little France Crescent
Edinburgh, EH16 4TJ, UK
Tel: +31 10 7043169
FAX: +31 10 7044743
Email: Elaine.Dzierzak@ed.ac.uk

Zhuan Li
Southern Medical University
School of Basic Medical Sciences
Department of Developmental Biology
Guangzhou, China
Email: lizhuan27@126.com

Key Points

1. Macrophages in the hindbrain-branchial arches region of the mouse embryo play a positive role in HS/PC expansion and/or maturation

2. Macrophages from embryonic head hematopoietic niches produce pro-inflammatory factor TNFα and enhance HS/PC expansion and/or maturation

Abstract

Along with the aorta-gonad-mesonephros region, the head is a site of hematopoietic stem and progenitor cell (HS/PC) development in the mouse embryo. Macrophages are present in both these embryonic hemogenic sites and recent studies indicate a functional interaction of macrophages with hematopoietic cells as they are generated in the aorta. Whereas, brain macrophages or 'microglia' are known to affect neuronal patterning and vascular circuitry in the embryonic brain, it is unknown whether macrophages play a role in head hematopoiesis. Here we characterize head macrophages and examine whether they affect the HS/PC output of the hindbrain-branchial arch (HBA) region of the mouse embryo. We show that HBA macrophages are $CD45^+F4/80^+CD11b^+Gr1^-$ and express the macrophage-specific *Csf1r-GFP* reporter. In the HBA of chemokine receptor deficient (*Cx3cr1$^{-/-}$*) embryos, a reduction in erythropoiesis is concomitant with a decrease in HBA macrophage percentages. In cocultures, we show that head macrophages boost HPC numbers from HBA endothelial cells >2-fold, and that the pro-inflammatory factor TNFα is produced by head macrophages and influences HBA hematopoiesis *in vitro*. Taken together, head macrophages play a positive role in HBA erythropoiesis and HS/PC expansion and/or maturation, acting as micro-environmental cellular regulators in hematopoietic development.

Introduction

Hematopoietic stem cells (HSC) are the self-renewing source of mature blood cell lineages in the adult. During embryonic development both hematopoietic progenitor cells (HPC) and HSCs are generated from endothelial cells of the major vasculature (aorta and vitelline/umbilical arteries)[1-4] through a specialized developmental process, endothelial-to-hematopoietic-transition (EHT) and emerge in the lumen as cell clusters. The mouse embryonic head also generates HSCs and HPCs [5] and functional hematopoietic assays localize these cells to the hindbrain and branchial arch (HBA) [6] vascular regions. Rather than the formation of hematopoietic clusters as in the embryonic aorta lumen, imaging analyses of the HBA reveal the close associations of only single hematopoietic cells adjacent to endothelial cells[6], suggesting differences in the regulation of head hematopoietic development.

Molecular studies on hematopoietic stem/progenitor cell (HS/PC) development in the aorta of zebrafish embryos and the aorta-gonad-mesonephros (AGM) region of mouse embryos identified some factors and signalling pathways that facilitate EHT[2,7-9]. Investigations focusing on the cellular micro-environment surrounding the embryonic aorta[10] revealed rare cell-cell interactions involving neutrophils[11] and macrophages[12,13]: In zebrafish embryos, neutrophils signal to the intra-aortic hematopoietic cells (IAHC) through TNFα and macrophages promote HS/PC mobilization at the vascular wall through localized production of MMP2/9[12,13]. A surprisingly large number of CD45$^+$F4/80$^+$ macrophages were found to be scattered around the mouse E10.5 aorta and adjacent to cells of the IAHC[8,14-16]. Recent time-lapse imaging studies show transient interactions of macrophages with IAHC [16].

The earliest embryonic macrophages in the mouse are formed in the yolk sac blood islands beginning at E7.5[17]. *In vivo* lineage tracing supports a recruitment of these macrophages to head region, where in the brain they become the tissue resident macrophages, 'microglia' that persist through all stages of life[18,19]. Microglia are regulators of central neural system patterning and promote vascular networking during embryonic stages[20-22]. During adult stages, macrophages are effectors of immune response homeostasis (pro- and anti-inflammatory). Macrophages express the transmembrane tyrosine kinase receptor (Csf1r)[23] and are regulated by colony stimulating factor-1 (Csf-1). *Csf1r*$^{-/-}$ mice exhibit diminished macrophage numbers, reproductive defects, obstructed organ development, and a severe brain phenotype (neocortical progenitor proliferation and apoptosis is increased, and the differentiation of some neuronal subtypes is reduced)[24,25]. While microglia-neuron interactions are thought to involve the Cx3cr1-Cx3cl1 chemokine signaling pathway[26], it

remains unknown whether macrophages/microglia are regulators of embryonic head hematopoiesis.

Pro-inflammatory factors produced by innate immune cells, such as Interleukin-1 (IL-1), interferons (IFN) and tumor necrosis factor α (TNFα) play a role in embryonic hematopoiesis[27]. In Zebrafish embryos, TNFα secreted by neutrophils activates downstream signalling pathways implicated in aortic HS/PC production[11]. IL1 receptor *(IL-1RI)*–deficient mouse embryos show a slight decrease in AGM HSC activity[28] in mouse and zebrafish embryos deficient for *IFN-γ* or *IFN-α* are significantly reduced in HS/PCs[15]. In this study, we examine the role of head macrophages in HS/PC development in the mouse embryonic HBA and report that they influence HBA erythropoiesis and promote expansion and/or maturation of HBA HS/PC through TNFα arising from HBA macrophages.

Materials and methods

Mouse and embryo generation. Wild type C57BL/6 and *MacGreen (Csf1r-GFP)*[29], Cx3cr1-GFP[30], Csf1r-Cre[31] (from J. W. Pollard), RosaDTAlox[32] (from G. Kassiotis) and *Vav-Cre* [33] (from N. Speck) mice (all C57BL/6-Ly5.2 background) were used for timed matings and C57BL/6-Ly5.1 mice (8-12 weeks) were transplantation recipients. Embryos were generated from *MacGreen* males crossed with wild type females, and *Csf1r-Cre* females crossed with *RosaDTA* males. Embryo staging was done by somite pair counts[34]. HBA were dissected [6] (Fig.1A) and forebrains used for pheno/genotyping. PCR primers used for genotyping embryos are in SupTable 1. Mice were housed in the University of Edinburgh animal facilities and experimentation complied with UK Home Office Regulations and Licensing.

Hematopoietic progenitor and stem cell assays. Single-cell suspensions from HBA or cultures were seeded in the Methylcellulose (M3434; Stem Cell Technologies) colony-forming unit-culture (CFU-C) assay, colonies counted after 10 days and lineage specific colony outputs quantitated as number of CFU-C per one embryo equivalent (ee) of HBA cells. HBA cells (1-3ee) were injected intravenously into (9.0Gy γ-irradiation, split dose) Ly5.1 mice. Peripheral blood was taken (4 and 16 wks) for Ly5.1-/Ly5.2-specific FACS analysis. Recipients are considered repopulated when ≥5% of cells are donor-derived.

OP9-DL1 coculture system. OP9-DL1-B1 (*Bmp4*$^{-/-}$) cells were generated by *CRISPR-Cas9* (*Bmp4* exon1 sg (single guide) RNA: 5'-*GTGTAAGGTTCGACGGACCG*-3', 5'*CGGTCCGTCGAACCTTACAC*-3'; *Bmp4* exon3 sgRNA: 5'-*ACCATCAGCATTCGGTTACC*-3', 5'-*GGTAACCGAATGCTGATGGT*-3') engineering. HBA cells were cocultured in 10% FBS (Hyclone, Brunschwig Chemie), α-MEM, 1%Pen-Strep,

1%Glutamax (all from Gibco) with OP9-DL1-B1 cells (SCF100ng/ml, IL3 100ng/ml and Flt3-ligand 100ng/ml; PeproTech) +/- CSF1R Inhibitor (BLZ945 6.7nM diluted in DMSO, MedChemExpress) [35]. TNFα, IL1β (PeproTech), TNFα neutralizing antibody (1µg/ml; R&D Systems) was added at the start of coculture. After 7 days, supernatant and semi-adhesive cells were harvested and sorted for ELISA assays and methylcellulose cultures, respectively.

Flow cytometry. Cells from HBA, cultures and adult hematopoietic tissues were antibody-stained (SupTable 2) for 30' on ice. Sorted cells were collected in 50% FBS/PBS for functional analyses or in lysis buffer for RNA extraction. Cytometry was performed on BDFortessa /AriaII (BD Biosciences).

Gene Expression Analysis. RNA from sorted cells was extracted with RNeasy MicroKit (Qiagen). cDNAs were generated with oligdT primers and SuperScriptIII Reverse Transcriptase (Thermo Fisher Scientific). RT-PCR were performed by using Fast SYBR™ Green Master Mix and ABI7900 (Thermo Fisher Scientific) detection. Primers are listed in SupTable 3.

Embryo Immunostaining. Wholemount staining was performed according to published methods[36]. *MacGreen* embryonic head was fixed 20' in 2% PFA. Antibodies are listed in SupTable 2.

Cytokine assays. TNFα protein concentration was tested with the BD™ Cytometric Bead Array (CBA) Kit. Standard curves were generated using supplied control samples and data analysed by FCAPArray™ software.

Statistical Analyses. Comparisons of 2 groups were performed with Student's t-test and comparison of more than 2 groups were performed using One-way ANOVA test. $p < 0.05$ was considered significant.

Results

<u>Phenotypic characterization of macrophages in the mouse embryonic HBA.</u> The hindbrain branchial (first and second) arch (HBA) region from *Csf1r-GFP* (*MacGreen,* macrophage reporter) transgenic mouse embryos was dissected (Fig.1A) and cells analysed by flow cytometry[19,24,29]. Brain-resident macrophages, microglia, originate from E7.5 yolk sac myeloid precursors and upon entry into the brain lose cKit expression and initiate F4/80 expression[19,37]. 99.6% of GFP$^+$ cells in the E10 HBA were positive for the hematopoietic marker CD45 (Fig.1B). Whereas >95% of these cells were CD11b$^+$F4/80$^+$, only a small

percentage were CD11b$^+$F4/80$^-$. Both fractions were negative for the granulocytic marker Gr1. Likewise, almost all (99.2%) CD45$^+$F4/80$^+$CD11b$^+$Gr1$^-$ cells were GFP$^+$ (Sup.Fig.1A). Thus, most HBA GFP$^+$ cells are macrophages. Between E9.5 and E10.5 there was a significant 3-fold increase in HBA GFP$^+$ cells (0.29±0.02% and 0.93±0.08%, respectively) which further increased to 1.13±0.23% at E11.5 (Fig.1C).

E10.5 *MacGreen* embryo wholemount images showed macrophages scattered throughout the HBA, with many macrophages localized around the CD31$^+$ endothelial cells of the large lateral vessels (Fig.1D, 1Di), the carotid arteries [6,38]. Macrophages also localized along the small vessels (not shown), consistent with a role for macrophages in vascular networking[22,39]. Macrophages were also present in the neuro-epithelium (Fig.1Dii).

Chemokine and chemokine receptor expression on HBA cells. Since chemokine receptor/ligand interactions are involved in inflammatory responses, we examined *MacGreen* HBA cells for the expression of Cx3cr1, Cxcr4, Cxcr2, Ccr7, Ccr5 and Ccr3. Flow cytometric analyses (Fig.1E, 1F) showed that >90% of GFP$^+$ cells expressed Cx3cr1 with a high mean fluorescence intensity (MFI, Sup.Fig.1B) and >85% expressed Cxcr4, but at a much lower MFI. About 78% of GFP$^+$ cells were Ccr3$^+$ (MFIs intermediate to high). Neither Ccr7 nor Cxcr2 were expressed, and <20% of cells were Ccr5$^+$. Hence, Cx3cr1, Cxcr4 and Ccr3 may be relevant to HBA macrophage signaling/function.

To examine whether distinct HBA cells expressed the ligands for these receptors, hematopoietic (HC; CD41$^+$ and/or CD45$^+$), endothelial (EC; CD31$^+$CD41$^-$CD45$^-$) and mesenchymal/other (MC; CD31$^-$CD41$^-$CD45$^-$) cells were sorted (Fig.2A) and qRT-PCR performed (Fig.2B). *Cx3cl1* expression was negligible in HCs and low in MCs, whereas expression in ECs was significantly higher than HCs. The expression of *Cxcl12* (ligand of Cxcr4) was significantly higher in MCs than in either ECs or HCs. *Ccl3* (ligand of Ccr1/Ccr5) was detected in both HCs and MCs, but not in ECs. *Ccl11* (ligand of Ccr3) was weakly expressed in MCs. Together, these results suggest that the Cx3cr1/Cx3cl1 and/or Cxcr4/Cxcl12 signalling axes may be active in the HBA, particularly in recruitment of macrophages to head ECs and/or MCs.

HBA macrophages and erythroid progenitors are quantitatively reduced in the absence of Cx3cr1. Cx3cr1 may be involved in the recruitment of yolk sac macrophage progenitors to the brain where they give rise to tissue resident microglia [37,39]. Given that >90% of HBA *MacGreen* macrophages express Cx3cr1 (Fig.1E), we tested whether deficiency of Cx3cr1 affects the percentage of macrophages in the HBA and whether HBA hematopoiesis is affected. The insertion of *EGFP* in the *Cx3cr1* gene reports *Cx3cr1* transcription while generating a null allele. No change in viable cell numbers in E10.5 *Cx3cr1$^{+/GFP}$* (HT) and

7

Cx3cr1$^{GFP/GFP}$ (KO) HBA were found as compared wild type (WT) HBA (SupTable 4). However, macrophage percentages in HT (0.73%±0.02%) and KO (0.38%±0.02%) HBA were significantly reduced (0.15-fold and 0.57-fold respectively) as compared to WT (0.86%±0.07%) (Fig.3A, 3B). Also, the percentage of phenotypic HPCs (cKit$^+$CD41^{low}) was decreased significantly to 0.42%±0.02% in HT and 0.32%±0.04% in KO HBA, as compared to WT (0.49%±0.09%) (Fig.3A, 3D, Sup.Fig.2). Functional assessment of the E10.5 HBA, demonstrated a significant reduction in the total number of CFU-Cs in KO HBA as compared to WT (Fig.3F). Evaluation of specific colony types revealed statistically significant decreases in erythroid colony numbers in the E10.5 KO HBA as compared to WT. Despite decreased percentages of macrophages (Fig.3C) in the E11.5 HBA, phenotypic HPCs were not reduced (Fig.3E) and CFU-C numbers in the KO were similar to those in the WT HBA (Fig.3G). These data suggest that Cx3cr1 dependent macrophages play a role in erythropoiesis in the HBA prior to or at E10.5, but not thereafter, implicating differential and/or temporal regulation of HBA hematopoiesis.

HBA macrophages promote the expansion and/or maturation of HBA EC-derived HPCs in OP9-DL1-B1 cocultures. As we previously reported, hematopoietic cells are generated from ECs in the embryonic head[5] and *in vitro* OP9-DL1 cocultures. To test the effect of head macrophages (MΦ) on head EC-derived hematopoiesis, we sorted HBA ECs (CD31$^+$CD41$^-$CD45$^-$) and HBA MΦ (CD45$^+$CD11b$^+$F480$^+$) (Sup.Fig.3A) and cocultured them on OP9-DL1-B1 (*Bmp4*$^{-/-}$) stromal cells (Fig.4A). E10.5 HBA (*VavCre* transgenic) ECs and WT HBA MΦ were used to validate the source of hematopoietic cells generated in the cultures. Following 7 days of OP9-DL1-B1 coculture, round semi-adherent clusters of hematopoietic cells were microscopically visible in the EC and EC+MΦ (MIX) cell cultures (Fig.4B). MΦ only cultures did not contain clusters, but 0.12±0.09x10^3 CD45$^+$ cells remained of the 1x10^3 input MΦ after 3 and 7 days of culture (Sup.Fig.3B). Whereas EC cultures contained 6.50±1.21x10^3 CD45$^+$ cells, MIX cultures showed 1.7-fold more CD45$^+$ cells (10.95±2.30x10^3) (Fig.4C) than the EC cultures, suggesting that MΦ addition increases hematopoiesis.

Sorted CD45$^+$ cells from the cultures were plated into methylcellulose culture to test for progenitor activity. After 7 days of MIX coculture, a significant 3.4-fold increase in CFU-C number (561.3±138.2 CFU-C/ee) was found as compared to EC cocultures (166.0±52.92 CFU-C/ee) (Fig.4D). We next analysed the DNA of individual CFU-C from the MIX cultures of *Vav-Cre* EC and WT CD45$^+$CD11b$^+$F4/80$^+$ MΦ to identify the source of the HPCs. Of the 40 CFU-Cs examined for the *Cre* transgene by PCR, all were positive, indicating that they were EC-derived (Sup.Fig.3C). No CFU-C originated from the MΦ. These data demonstrate that HBA MΦ promote an increase in EC-derived HPCs *in vitro*.

HBA macrophage depletion influences HS/PC numbers. Using the rationale that >95% of HBA MΦ are Csf1r expressing (Fig.1B) and that Csf1r is not expressed by HSCs or some HPCs in the midgestation embryo [40,41] or as we found by 36% of HBA HPCs (Sup.Fig.4B), the Csf1r inhibitor BLZ945 was added to the MIX cultures to test whether MΦ depletion affects HBA HPC numbers. Whereas the number of CD45^{+} hematopoietic cells showed little change between BLZ945-treated and vehicle-treated control MIX cultures (Fig.4E), the number of CFU-C was significantly reduced in the BLZ945-treated MIX cultures and was similar to EC-only cultures, as compared to the control MIX cultures (Fig.4F). These results suggest that the *in vitro* increase in HBA HPCs is dependent on MΦ.

To further examine HBA hematopoiesis *in vivo* in the absence of MΦ, *Csf1r-Cre* mice were crossed with *RosaDTA* mice (*lox-stop-lox-diphtheria toxin A*). Normal Mendelian ratios of *Csf1r-Cre:DTA* and WT midgestation embryos were found (SupTable 5). The total viable HBA cell number was comparable between *Csf1r-Cre:DTA* and WT siblings (SupTable 6), and viable cell percentages similar in E9.5 to E11.5 HBA (Sup.Fig.4; Fig.5A). Whereas CD31^{+}CD45^{-} EC percentages were unaffected (Fig.5C) in the E9.5 to E11.5 *Csf1r-Cre:DTA* HBA and hematopoietic-related gene expression was not affected (E10.5; Sup.Fig.4E), MΦ (CD45^{+}CD11b^{+}F480^{+}) were almost completely absent (Fig.5B), indicating the specificity of targeted ablation. Interestingly, the percentage of phenotypic HCs (CD45^{+}CD11b^{-}F4/80^{-}; excludes macrophages) was decreased in the E9.5 to E11.5 *Csf1r-Cre:DTA* HBA, compared with the WT siblings (Fig.5D). CFU-C assays confirmed a decrease in functional HPC, with 3.0±3.0 CFU-C per E9.5 *Csf1r-Cre:DTA* HBA as compared to 73.3±18.3 CFU-C per WT HBA. Similar decreases in CFU-Cs were found in the E10.5 and E11.5 *Csf1r-Cre:DTA* HBA (38.5±5.3, 18.0±9.9 per HBA, respectively) compared with control (155.0±47.7, 503±41.8 per HBA) (Fig.5E). These results, together with the results of the coculture system suggest that macrophages have a positive influence on the expansion and/or maturation of HPCs in the HBA.

In vivo transplantation assays were performed with cells from E11.5 *Csf1r-Cre:DTA* HBA to test whether macrophages are involved in HSC development. Whereas the peripheral blood donor cell chimerism in 3 of 8 mice injected with WT HBA cells was >5% at 4 weeks post-transplantation and averaged 22.7±12.3% at 16 weeks post-transplantation, no recipients (0 of 8; n=5) receiving *Csf1r-Cre:DTA* HBA cells were donor cell-engrafted (Fig.5F). These data support a role for macrophages in HS/PC expansion and/or maturation in the HBA.

Pro-inflammatory signalling molecules are expressed by HBA cells. Macrophages may function in the HBA through the local secretion of pro-inflammatory factors such as IL1 and TNFα, which have been shown by others to be involved in embryonic hematopoiesis[11,28]. To

examine pro-inflammatory factor expression in the HBA (*MacGreen* embryos), qRT-PCR was performed for *IL1α*, *IL1β*, *TNFα* and *IL-6* on GFP$^+$ cells (mostly macrophages, Fig.1B), other HBA cells (GFP$^-$) and control OP9-DL1-B1 cells. *IL1α*, *IL1β* and *TNFα* were expressed exclusively by GFP$^+$ cells, while IL-6 expression was restricted to OP9-DL1 cells (Fig.6A). Expression was also examined in EC (CD31$^+$CD45$^-$) and MΦ (CD45$^+$CD11B$^+$F480$^+$GFP$^+$) (Fig.6B). *IL1α*, *IL1β* and *TNFα* expression was confirmed in MΦ and only low/no expression in EC. If these pro-inflammatory factors are involved in the EHT process or hematopoietic growth, receptor expression would be expected on HBA EC or HC. According to the gating strategy in Fig.2A, MC (mesenchymal cells/other), ECs and HCs were sorted and tested for expression of *IL1* receptors (*IL1R1*, *IL1Rap*, *IL1R2*) and *TNFα* receptors (*TNFR1*, *TNFR2*). All three HBA populations expressed *IL1R1* and *IL1Rap*. *IL1R2* was highly expressed in HCs, with very little/no expression in MCs and ECs. *TNFR1* expression was 4.2-fold higher in ECs as compared to MCs and 2.2-fold higher than HCs. In contrast, *TNFR2* was expressed highly in HCs (Fig.6C). These results showing expression of *IL1R1*, *IL1Rap and TNFR1* on HBA ECs and *TNFR2* on HCs suggest that they may respond to MΦ-derived IL1β and TNFα.

Supernatants from cocultures were tested for the presence of pro-inflammatory factors TNFα and IL1β. ELISA analysis showed quantitatively higher levels of *TNFα* in the MΦ only (2511.0±668.9fg/ml) and MIX (2049.0±188.3fg/ml) cultures compared to EC (371.3±231.1fg/ml) cultures (Fig.7A). Only very low levels of IL1β protein were found in the three cultures (data not shown). Hence, macrophage-produced TNFα may induce HS/PC generation and/or maturation in the mouse HBA.

Pro-inflammatory factor TNFα addition to HBA EC cultures increases HPC numbers.
To test whether TNFα could substitute for HBA MΦ, TNFα was titrated into HBA EC cultures. After 7 days, CD45$^+$ cell numbers were not significantly changed in 1ng/ml or 10ng/ml TNFα-supplemented cultures as compared to the no-TNFα cultures, but were reduced in 50ng/ml TNFα cultures (Fig.7B). However, significant increases in CFU-C numbers (1073.0±225.9 and 931.7±67.6 respectively) were found in cultures with 1ng/ml or 10ng/ml TNFα, compared to no-TNFα cultures (557.6±68.2). 50ng/ml TNFα cultures yielded similar CFU-C to cultures without TNFα (Fig.7C).

To validate the effect of TNFα we added TNFα neutralizing antibody (nAb) to EC and MIX cultures. CD45$^+$ cell and CFU-C numbers did not change in the EC cultures in the presence of the nAb (Fig7D, 7E). In contrast, addition of nAb to MIX cultures showed a significant reduction in CFU-C numbers (659.0±80.6), as compared to MIX (933.9±62.1) and EC + TNFα (931.7±67.6) control cultures (Fig.7E). These results suggest that TNFα-secreting MΦ

promote expansion and/or maturation of HPCs (mostly GM progenitors) derived from HBA ECs.

Discussion

Our identification of a novel role for macrophages in hematopoiesis in the developing HBA now adds to the known roles of macrophages in the embryonic head, such as vascular networking by tip fusion of endothelial cells[22] and neuronal interactions and patterning[42,43]. Interestingly Cx3cr1/Cx3cl1 axis is involved all these developmental processes. Macrophages influence the expansion and/or maturation of HBA HS/PCs, and likely regulate this process through production of TNFα. Although some pro-inflammatory molecules were shown previously to affect the emergence of HS/PCs in the aorta region of zebrafish and mouse embryos[11,15], this is the first demonstration that macrophages are important cellular regulators of embryonic head hematopoiesis. As macrophages are involved in neuronal patterning of the embryonic brain[21], our results from early hematopoietic developmental stages may have biomedical relevance for neuropathologies during later life stages.

Macrophages in the embryonic HBA regulate hematopoiesis *in vivo*. As well as expressing macrophage markers CD11b, F4/80 and CD45, all midgestation HBA macrophages express the *Csf1r-GFP* reporter. *Csf1r*-expressing cells were found in close proximity to the CD31$^+$ brain vasculature and by flow cytometry were found to express high levels of the Cx3cr1, Cxcr4 and Ccr3 chemokine receptors. Interestingly, HBA endothelial cells express *Cx3cl1*, the ligand for Cx3cr1.

It has been shown that emigration of yolk sac-derived macrophages to the embryonic brain [18,19] and to the AGM [16] is dependent on the Cx3cr1/Cx3cl1 signaling axis. Hematopoietic cells in the aorta during the time of endothelial-to-hematopoietic transition are decreased/absent in the absence of Cx3cr1, and AGM HPC numbers and HSC *in vivo* repopulating activity are decreased in *Cx3cr1* null embryos [16] . Similarly, we found that HPC numbers in the HBA of *Cx3cr1* null embryos were significantly reduced. This is likely to be a consequence of decreased macrophage emigration to this region and is supported by the fact that macrophage (CD45$^+$CD11b$^+$F4/80$^+$) percentages were significantly (50%) reduced and percentages of progenitor cells (cKit$^+$CD41^{low}) were also significantly reduced in the *Cx3cr1* null HBA.

We also examined the role of macrophages in HBA hematopoiesis by Cre-Lox targeting DTA-mediated ablation to Csf1r$^+$ macrophages. HPC numbers in the *Csf1r-DTA* HBA were

significantly reduced as compared to numbers in WT littermate HBAs. Moreover, no transplantable HSCs were found in *Csf1r-DTA* HBAs. It is important to note that there was a complete absence of CD45^{+}CD11b^{+}F4/80^{+} macrophages in the *Csf1r-DTA* HBA, but viable cells and CD31^{+}CD45^{-} EC percentages were largely unaffected.

Since Csf1r is expressed on multilineage (B, T and myeloid) progenitors in the embryo it has been suggested that this receptor plays a role in early hematopoiesis [44,45]. Others have recently reported that Csf1r is expressed by and regulates myeloid-primed B-lymphoid progenitors in the mouse fetal liver [46]. Single cell RNAsequencing of highly enriched HS/PCs from mouse embryonic and fetal stages reveal some low Csf1r expression on these cells[47], yet Csf1r cell tracing and other studies suggest that Csfr1 is not expressed by HSCs [16,41]. Thus, it is unclear in the HBA, whether cells other than macrophages express Csf1r. Our analysis of sorted MacGreen HBA cells revealed that HPCs were distributed in the high, intermediate and negative expressing fractions (Sup.Fig.4A) and thus, has implications for the use of the *in vivo* Csf1r targeted DTA ablation model. Within E10.5 HBA, 36% of HPC are Csfr1 negative, 28% are intermediate-expressing and 36% are high-expressing. If DTA is directly ablating the high and intermediate expressing HPCs, we would expect to find a 64% decrease in the number of CFU-C/HBA. However, a 78% decrease in CFU-C/HBA was found (Fig.5E), leaving open the possibility that some Csf1r negative HPCs are affected by the absence of macrophages. Further studies are needed to address this.

As compared to DTA-mediated macrophage ablation, which resulted in large reductions in CFU-C numbers/HBA, deficiency of *Cx3cr1* had a mild effect, reducing CFU-C numbers by only 10%. The differences are likely due the fact that in addition to Cx3cr1/Cx3cl1, several other chemokines/ligands are playing roles in recruiting macrophages/progenitors to the HBA. Indeed, not only is Cx3cr1 and its ligand expressed in macrophages and ECs respectively, but Cxcr4 and its ligand Cxcl12 respectively are expressed in macrophages and MCs of embryonic head. The Cxcr4/Cxcl12 axis maintains the HSC pool in the adult bone marrow, and hence it may play an HS/PC maintenance role in the HBA.

Macrophages promote increases in HPC numbers from HBA endothelial cells *in vitro*.
Vascular structures in the embryonic head are complex. Unlike the aorta, in which hematopoietic cell clusters have been found in close association with the vascular endothelium, only single hematopoietic cells have been found in association with the embryonic head vasculature[6,48]. Three-dimensional composite images of the whole *Csf1r-GFP* embryonic head, show a close association of GFP^{+} macrophages with CD31^{+}CD45^{-} ECs, suggesting an influence of macrophages in the HBA *in vivo*. We used an *in vitro* coculture system to test for the effects of macrophages on hematopoietic cells and HPCs

arising from HBA ECs. Like aortic ECs, cultures of HBA ECs show that the head vasculature produces HS/PC. A significant 3-fold increase in HPCs in MΦ+EC (MIX) cocultures was found, as compared to ECs alone. When a Csf1r inhibitor was added, it blocked the promotion of HPC expansion. This could be due to the direct effects of the inhibitor on macrophages or may be due to direct effects of the inhibitor on Csfr1 expressing HPCs. Interestingly, the same number of CFU-C/HBA was found as those produced by the EC-only cultures, thus the HBA contains some Csf1r independent HPC. The interaction of HBA macrophages with HBA EC may, in addition to increasing HPC numbers, influence EC hematopoietic fate induction. We have attempted to examine this issue in the OP9-DL1-B1 MIX and EC cultures. Preliminary results indicate that the number of hematopoietic-like clusters generated after 3 or 7 days of MIX cultures increases by a factor of 2 compared to the EC cultures (the number of cells per cluster does not change). Continuous vital imaging of EC and HC at the single cell level in MIX cultures is necessary to resolve this issue.

Actions of pro-inflammatory factors on HBA hematopoiesis. Within the cells of the HBA, we found that the pro-inflammatory factor TNFα was most highly and specifically expressed by macrophages. HBA ECs express their cognate receptors. Supplementation of HBA EC cultures with TNFα resulted in more HPCs: HPC numbers were increased to the same degree as when macrophages were added to the culture. Moreover, a TNFα blocking antibody when added to the MIX cocultures, reduced HPC numbers to those found in EC only cocultures. Our data is consistent with a previous report in which TLR stimulations in embryos resulted in the secretion of cytokines including TNFα, from macrophages[49]. Other groups have shown that neutrophil-derived TNFα in zebrafish embryos is required for HS/PC specification[11], and that TNFα in adult mouse bone marrow granulocytes promotes vascular and hematopoietic regeneration[50]. However, the role for the TNF signalling pathway in HSC maintenance is controversial. In a TNF loss-of-function *in vivo* model, one group showed that TNF plays a stimulatory function on HSC maintenance[51]. In contrast, another group showed that TNF is a suppressor of normal HSC activity *in vitro* and *in vivo*[52-55]. In our coculture system, the observed positive influence of TNFα on CD45$^+$ cell numbers is concentration dependent: Low and intermediate concentrations of TNFα increased CFU-C number/HBA, whereas a high concentration showed the same CFU-C number/HBA as in the absence of TNFα. Thus, the concentration of active TNFα may explain the conflicting results in the literature. In the HBA, it is likely that TNFα exerts its positive influence on the HPC *in vitro* through factor concentration gradients elicited through the direct interaction with or proximity of macrophages.

Along with IL1β which we have shown here is expressed by HBA macrophages, factors such as *IFNγ* and prostaglandin E2 that have been shown to regulate HSC production of zebrafish and mouse AGM HSCs[15,56,57] would be interesting to examine in the HBA for effects on endothelial to hematopoietic transition and HPC function. Together with transcriptome profiling of HBA macrophages, it may be possible to identify the combination and balance of different factors regulating hematopoiesis at different sites of embryonic development.

Acknowledgements

Authorship Contributions

E.Dzierzak and Z. Li conceived the project and designed the experiments. S. Mariani provided some reagents, helped design some experiments and discussed data. C. Rodriguez-Seoane performed some qRT-PCR, FACS and progenitor and transplantation experiments and discussed data. W. He and X. Ning helped perform some coculture experiments. C.S. Vink performed irradiations and B. Liu gave material support. E. Dzierzak and Z. Li wrote the manuscript.

Disclosures

The authors have no conflicts of interest to disclose.

References

1.   Muller AM, Medvinsky A, Strouboulis J, Grosveld F, Dzierzak E. Development of hematopoietic stem cell activity in the mouse embryo. *Immunity*. 1994;1(4):291-301.
2.   Chen MJ, Yokomizo T, Zeigler BM, Dzierzak E, Speck NA. Runx1 is required for the endothelial to haematopoietic cell transition but not thereafter. *Nature*. 2009;457(7231):887-891.
3.   Boisset JC, van Cappellen W, Andrieu-Soler C, Galjart N, Dzierzak E, Robin C. In vivo imaging of haematopoietic cells emerging from the mouse aortic endothelium. *Nature*. 2010;464(7285):116-120.
4.   Yokomizo T, Ng CE, Osato M, Dzierzak E. Three-dimensional imaging of whole midgestation murine embryos shows an intravascular localization for all hematopoietic clusters. *Blood*. 2011;117(23):6132-6134.
5.   Li Z, Lan Y, He W, et al. Mouse embryonic head as a site for hematopoietic stem cell development. *Cell Stem Cell*. 2012;11(5):663-675.
6.   Li Z, Vink CS, Mariani SA, Dzierzak E. Subregional localization and characterization of Ly6aGFP-expressing hematopoietic cells in the mouse embryonic head. *Dev Biol*. 2016;416(1):34-41.
7.   Solaimani Kartalaei P, Yamada-Inagawa T, Vink CS, et al. Whole-transcriptome analysis of endothelial to hematopoietic stem cell transition reveals a requirement for Gpr56 in HSC generation. *J Exp Med*. 2015;212(1):93-106.
8.   Eich C, Arlt J, Vink CS, et al. In vivo single cell analysis reveals Gata2 dynamics in cells transitioning to hematopoietic fate. *J Exp Med*. 2018;215(1):233-248.
9.   Thambyrajah R, Mazan M, Patel R, et al. GFI1 proteins orchestrate the emergence of haematopoietic stem cells through recruitment of LSD1. *Nat Cell Biol*. 2016;18(1):21-32.
10.   Tamplin OJ, Durand EM, Carr LA, et al. Hematopoietic stem cell arrival triggers dynamic remodeling of the perivascular niche. *Cell*. 2015;160(1-2):241-252.
11.   Espin-Palazon R, Stachura DL, Campbell CA, et al. Proinflammatory signaling regulates hematopoietic stem cell emergence. *Cell*. 2014;159(5):1070-1085.
12.   Travnickova J, Tran Chau V, Julien E, et al. Primitive macrophages control HSPC mobilization and definitive haematopoiesis. *Nat Commun*. 2015;6:6227.
13.   Theodore LN, Hagedorn EJ, Cortes M, et al. Distinct Roles for Matrix Metalloproteinases 2 and 9 in Embryonic Hematopoietic Stem Cell Emergence, Migration, and Niche Colonization. *Stem Cell Reports*. 2017;8(5):1226-1241.
14.   Yokomizo T, Dzierzak E. Three-dimensional cartography of hematopoietic clusters in the vasculature of whole mouse embryos. *Development*. 2010;137(21):3651-3661.
15.   Li Y, Esain V, Teng L, et al. Inflammatory signaling regulates embryonic hematopoietic stem and progenitor cell production. *Genes Dev*. 2014;28(23):2597-2612.
16.   Mariani SA, Li Z, Rice S, et al. Pro-inflammatory Aorta-Associated Macrophages Are Involved in Embryonic Development of Hematopoietic Stem Cells. *Immunity*. 2019;50(6):1439-1452 e1435.
17.   Palis J, Robertson S, Kennedy M, Wall C, Keller G. Development of erythroid and myeloid progenitors in the yolk sac and embryo proper of the mouse. *Development*. 1999;126(22):5073-5084.
18.   Goldmann T, Wieghofer P, Jordao MJ, et al. Origin, fate and dynamics of macrophages at central nervous system interfaces. *Nat Immunol*. 2016;17(7):797-805.
19.   Ginhoux F, Greter M, Leboeuf M, et al. Fate mapping analysis reveals that adult microglia derive from primitive macrophages. *Science*. 2010;330(6005):841-845.
20.   Frost JL, Schafer DP. Microglia: Architects of the Developing Nervous System. *Trends Cell Biol*. 2016;26(8):587-597.
21.   Salter MW, Stevens B. Microglia emerge as central players in brain disease. *Nat Med*. 2017;23(9):1018-1027.
22.   Fantin A, Vieira JM, Gestri G, et al. Tissue macrophages act as cellular chaperones for vascular anastomosis downstream of VEGF-mediated endothelial tip cell induction. *Blood*. 2010;116(5):829-840.

23.   Stanley ER, Chitu V. CSF-1 receptor signaling in myeloid cells. *Cold Spring Harb Perspect Biol*. 2014;6(6).

24.   Erblich B, Zhu L, Etgen AM, Dobrenis K, Pollard JW. Absence of colony stimulation factor-1 receptor results in loss of microglia, disrupted brain development and olfactory deficits. *PLoS One*. 2011;6(10):e26317.

25.   Nandi S, Gokhan S, Dai XM, et al. The CSF-1 receptor ligands IL-34 and CSF-1 exhibit distinct developmental brain expression patterns and regulate neural progenitor cell maintenance and maturation. *Dev Biol*. 2012;367(2):100-113.

26.   Wolf Y, Yona S, Kim KW, Jung S. Microglia, seen from the CX3CR1 angle. *Front Cell Neurosci*. 2013;7:26.

27.   Wajant H, Pfizenmaier K, Scheurich P. Tumor necrosis factor signaling. *Cell Death Differ*. 2003;10(1):45-65.

28.   Orelio C, Haak E, Peeters M, Dzierzak E. Interleukin-1-mediated hematopoietic cell regulation in the aorta-gonad-mesonephros region of the mouse embryo. *Blood*. 2008;112(13):4895-4904.

29.   Sasmono RT, Williams E. Generation and characterization of MacGreen mice, the Cfs1r-EGFP transgenic mice. *Methods Mol Biol*. 2012;844:157-176.

30.   Jung S, Aliberti J, Graemmel P, et al. Analysis of fractalkine receptor CX(3)CR1 function by targeted deletion and green fluorescent protein reporter gene insertion. *Mol Cell Biol*. 2000;20(11):4106-4114.

31.   Deng L, Zhou JF, Sellers RS, et al. A novel mouse model of inflammatory bowel disease links mammalian target of rapamycin-dependent hyperproliferation of colonic epithelium to inflammation-associated tumorigenesis. *Am J Pathol*. 2010;176(2):952-967.

32.   Marques R, Williams A, Eksmond U, et al. Generalized immune activation as a direct result of activated CD4+ T cell killing. *J Biol*. 2009;8(10):93.

33.   Stadtfeld M, Ye M, Graf T. Identification of interventricular septum precursor cells in the mouse embryo. *Dev Biol*. 2007;302(1):195-207.

34.   Medvinsky A, Taoudi S, Mendes S, Dzierzak E. Analysis and manipulation of hematopoietic progenitor and stem cells from murine embryonic tissues. *Curr Protoc Stem Cell Biol*. 2008;Chapter 2:Unit 2A 6.

35.   Pyonteck SM, Akkari L, Schuhmacher AJ, et al. CSF-1R inhibition alters macrophage polarization and blocks glioma progression. *Nat Med*. 2013;19(10):1264-1272.

36.   Yokomizo T, Yamada-Inagawa T, Yzaguirre AD, Chen MJ, Speck NA, Dzierzak E. Whole-mount three-dimensional imaging of internally localized immunostained cells within mouse embryos. *Nat Protoc*. 2012;7(3):421-431.

37.   Mass E, Ballesteros I, Farlik M, et al. Specification of tissue-resident macrophages during organogenesis. *Science*. 2016;353(6304).

38.   Kaufman MH. The Atlas of Mouse Development. London: Elsevier Academic Press; 1992.

39.   Stremmel C, Schuchert R, Wagner F, et al. Yolk sac macrophage progenitors traffic to the embryo during defined stages of development. *Nat Commun*. 2018;9(1):75.

40.   Mariani SA, Li Z, Rice S, et al. A novel embryonic macrophage subset functions in the hematopoietic stem cell-generative microenvironment. 2019:Accepted.

41.   Tarnawsky SP, Yoshimoto M, Deng L, Chan RJ, Yoder MC. Yolk sac erythromyeloid progenitors expressing gain of function PTPN11 have functional features of JMML but are not sufficient to cause disease in mice. *Dev Dyn*. 2017;246(12):1001-1014.

42.   Fuhrmann M, Bittner T, Jung CK, et al. Microglial Cx3cr1 knockout prevents neuron loss in a mouse model of Alzheimer's disease. *Nat Neurosci*. 2010;13(4):411-413.

43.   Kierdorf K, Prinz M. Factors regulating microglia activation. *Front Cell Neurosci*. 2013;7:44.

44.   Boiers C, Carrelha J, Lutteropp M, et al. Lymphomyeloid contribution of an immune-restricted progenitor emerging prior to definitive hematopoietic stem cells. *Cell Stem Cell*. 2013;13(5):535-548.

45.   Kajikhina K, Melchers F, Tsuneto M. Chemokine polyreactivity of IL7Ralpha+CSF-1R+ lympho-myeloid progenitors in the developing fetal liver. *Sci Rep*. 2015;5:12817.

46.   Zriwil A, Boiers C, Wittmann L, et al. Macrophage colony-stimulating factor receptor marks and regulates a fetal myeloid-primed B-cell progenitor in mice. *Blood*. 2016;128(2):217-226.

47.   Zhou F, Li X, Wang W, et al. Tracing haematopoietic stem cell formation at single-cell resolution. *Nature*. 2016;533(7604):487-492.

48.   Iizuka K, Yokomizo T, Watanabe N, et al. Lack of Phenotypical and Morphological Evidences of Endothelial to Hematopoietic Transition in the Murine Embryonic Head during Hematopoietic Stem Cell Emergence. *PLoS One*. 2016;11(5):e0156427.

49.   Balounova J, Vavrochova T, Benesova M, Ballek O, Kolar M, Filipp D. Toll-like receptors expressed on embryonic macrophages couple inflammatory signals to iron metabolism during early ontogenesis. *Eur J Immunol*. 2014;44(5):1491-1502.

50.   Bowers E, Slaughter A, Frenette PS, Kuick R, Pello OM, Lucas D. Granulocyte-derived TNFalpha promotes vascular and hematopoietic regeneration in the bone marrow. *Nat Med*. 2017.

51.   Rebel VI, Hartnett S, Hill GR, Lazo-Kallanian SB, Ferrara JL, Sieff CA. Essential role for the p55 tumor necrosis factor receptor in regulating hematopoiesis at a stem cell level. *J Exp Med*. 1999;190(10):1493-1504.

52.   Bryder D, Ramsfjell V, Dybedal I, et al. Self-renewal of multipotent long-term repopulating hematopoietic stem cells is negatively regulated by Fas and tumor necrosis factor receptor activation. *J Exp Med*. 2001;194(7):941-952.

53.   Dybedal I, Bryder D, Fossum A, Rusten LS, Jacobsen SE. Tumor necrosis factor (TNF)-mediated activation of the p55 TNF receptor negatively regulates maintenance of cycling reconstituting human hematopoietic stem cells. *Blood*. 2001;98(6):1782-1791.

54.   Milsom MD, Schiedlmeier B, Bailey J, et al. Ectopic HOXB4 overcomes the inhibitory effect of tumor necrosis factor-{alpha} on Fanconi anemia hematopoietic stem and progenitor cells. *Blood*. 2009;113(21):5111-5120.

55.   Pronk CJ, Veiby OP, Bryder D, Jacobsen SE. Tumor necrosis factor restricts hematopoietic stem cell activity in mice: involvement of two distinct receptors. *J Exp Med*. 2011;208(8):1563-1570.

56.   Hoggatt J, Singh P, Sampath J, Pelus LM. Prostaglandin E2 enhances hematopoietic stem cell homing, survival, and proliferation. *Blood*. 2009;113(22):5444-5455.

57.   North TE, Goessling W, Walkley CR, et al. Prostaglandin E2 regulates vertebrate haematopoietic stem cell homeostasis. *Nature*. 2007;447(7147):1007-1011.

Figure Legends

Figure 1. Characterization of macrophages in E9.5 to E11.5 *MacGreen* HBA. (A) Schematic diagram of dissected hindbrain-branchial arch (HBA) region on the mouse embryonic head. The region includes the 1st and 2nd branchial arches. (B) Flow cytometric profile for E10.5 *MacGreen* HBA cells showing that all GFP$^+$ (high-expressing) cells are CD45$^+$CD11b$^+$F4/80$^+$Gr1$^-$ macrophages. Percentages shown in gated areas. FSC=forward scatter. (C) Percentages of *MacGreen* GFP$^+$ cells in E9.5, E10.5 and E11.5 HBA (n≥3). *p=0.016, ***p<0.001. (D) Three-dimensional whole-mount images of an immunostained *MacGreen* E10.5 head (34 somite pairs (sp)), with boxed areas enlarged in right panels. Anti-GFP (green) and anti-CD31 (magenta) antibody staining shows localization of macrophages surrounding the CD31$^+$ vasculature. CA=carotid artery, V=brain ventricle, NE=neuro-epithelium. Bar=10 μm. (E) Representative flow cytometric data showing mean fluorescence intensity (MFI) and percentage of GFP$^+$ macrophages and GFP$^-$ cells expressing chemokine receptors in the E10.5 (32-39 sp) *MacGreen* HBA. Dotted line=FMO, dashed line=GFP$^-$ cells and black line with grey filled=GFP$^+$ cells. (F) Bar graphs showing percentages of chemokine receptor-expressing cells in the GFP$^+$ fraction. n=4 for Cx3cr1, Ccr7, Ccr5, Ccr3 and n=3 for Cxcr4, Cxcr2.

Figure 2. HBA cell subset-specific expression of chemokines at E10.5. (A) Flow cytometric sorting strategy for enrichment of mesenchymal/other cells (MC; CD31$^-$CD41$^-$CD45$^-$), endothelial cells (EC: CD31$^+$CD41$^-$CD45$^-$) and hematopoietic cells (HC; CD41$^+$ and/or CD45$^+$). (B) Relative expression of mRNA for chemokine genes *Cx3cl1, Cxcl12, Ccl3* and *Ccl11* as normalized to *actin* in E10.5 HBA sorted MC, EC and HC. SEM is shown. n=5, *p<0.05, **p<0.01.

Figure 3. *Cx3cr1* deficiency leads to the reduction of hematopoietic progenitors in E10.5 HBA, but not in E11.5 HBA. (A) Representative flow cytometric data and gated areas showing percentages of CD45$^+$ hematopoietic cells, cKit$^+$CD41^{low} hematopoietic progenitor cells, GFP$^+$CD45$^+$ cells and GFP$^+$CD45$^+$CD11b$^+$F4/80$^+$ macrophages in the HBA of *Cx3cr1$^{+/+}$* (wild type=WT), *Cx3cr1$^{+/GFP}$* (heterozygous mutants=HT) and *Cx3cr1$^{GFP/GFP}$* (knockout=KO) E10.5 littermates. The percentage of CD45$^+$CD11b$^+$F4/80$^+$ macrophages in the WT, HT and KO HBA of (B) E10.5 (31-39 sp) and (C) E11.5 (42-48 sp) embryos. Each square represents a single HBA, n=4, **p<0.01, ***p<0.001. The percentage of cKit$^+$CD41^{low} progenitor cells in WT, HT and KO HBA of (D) E10.5 and (E) E11.5 littermates. n=4, *p=0.026, **p=0.006. Methylcellulose culture data showing the number of CFU-Cs per 1 embryo equivalent (ee) of E10.5 (F) and E11.5 (G) WT, HT and KO HBA cells. n=3,

*p=0.047. Numbers of each colony type are indicated by bar color. CFU-C=colony forming unit-cell; GEMM= granulocyte, erythroid, macrophage, megakaryocyte; GM=granulocyte, macrophage; M=macrophage; G=granulocyte; E=erythroid.

Figure 4. HBA macrophages increase number of HBA EC-derived HPCs. (A) Schematic diagram of the coculture system, with a monolayer of OP9-DL1-B1 cells overlaid with HBA endothelial cells (EC), HBA macrophages (MΦ) or EC+ MΦ (MIX). One embryo equivalent of HBA ECs (CD31$^+$CD41$^-$CD45$^-$) and/or 1,000 HBA MΦ (CD45$^+$CD11b$^+$F480$^+$) were added to each coculture well. After 7 days, non-adherent cells were harvested, FACS sorted and plated in methylcellulose to quantitate hematopoietic colonies (CFU-C). The genotype of each colony was determined by *Cre* PCR. (B) Bright field microscopic images show the round morphology and density of hematopoietic cells after 7 days of OP9-DL1-B1 culture of EC, MΦ or MIX. The number of (C) CD45$^+$ cells and (D) CFU-Cs per ee of E10.5 (31-35 sp) HBA cells after 7 days of OP9-DL1-B1 culture of EC, MΦ or MIX. n=4, *p<0.05. The number of (E) CD45$^+$ cells and (F) CFU-Cs per ee of E10.5 HBA from OP9-DL1-B1 culture of EC and MIX with or without Csf1r inhibitor BLZ945 (6.7nM). BLZ945 (BLZ) is diluted in DMSO. EC$^\&$ and MIX$^\&$ have the DMSO$^\&$ diluent added as a vehicle control. SEM is shown. n=3, *p<0.05. ee=embryo equivalent. Colony types indicated by color bars.

Figure 5. Hematopoietic stem/progenitor cells are reduced in the E9.5 to E11.5 HBA in Csf1r-directed DTA depletion. Percentages of (A) viable HBA cells as determined by Hoescht dye exclusion, (B) CD45$^+$F480$^+$CD11b$^+$ macrophages, (C) CD31$^+$CD45$^-$ endothelial cells and (D) CD45$^+$F4/80$^-$CD11b$^-$ hematopoietic cells from E9.5 to E11.5 wild type (WT) and *Csf1r-Cre$^{+/DTA}$* (*Cre$^{+/DTA}$*) littermates in FACS analysis. Each dot or square represents one WT or *Cre$^{+/DTA}$* embryo. SEM is shown. n=3, *p<0.05, ***p<0.001. MΦ=macrophages; EC=endothelial cells; HC=hematopoietic cells. (E) CFU-C per embryo equivalent (ee) of HBA cells in E9.5, 10.5 and 11.5 WT and *Cre$^{+/DTA}$* littermates. Colony type is indicated by color bars. E9.5 n=2, E10.5 n=3, E11.5 n=3, *p<0.05, ***p<0.001. (F) Percentage of donor-cell (Ly5.2) chimerism in the peripheral blood of irradiated (Ly5.1) recipients injected with WT or *Cre$^{+/DTA}$* E11.5 (44-48 sp) HBA cells as determined by Ly5.1/Ly5.2 FACS analysis. Eight recipients received WT (1-3 ee) and 8 recipients received *Cre$^{+/DTA}$* (1-3) HBA cells. Dots and squares indicate individual recipients of WT or *Cre$^{+/DTA}$* cells respectively that were examined at 4 and 16 weeks (W) post-transplantation. n=5.

Figure 6. Genes of proinflammatory pathways are expressed in HBA cells. (A) Relative mRNA expression of *IL1α, IL1β, TNFα* and *IL-6* normalized to *actin* in GFP$^+$ (G$^+$) and GFP$^-$ (G$^-$) cells in the E10.5 *MacGreen* HBA as determined by qRT-PCR. OP9-DL1-B1 (DL1) is the negative control. n=3, *p<0.05. (B) Relative mRNA expression of *IL1α, IL1β, TNFα* and *IL-6*

as normalized to *actin* in macrophages (MΦ, CD45⁺CD11b⁺F4/80⁺Gr1-), endothelial cells (EC, CD31⁺CD45⁻) in the E10.5 HBA as determined by qRT-PCR. OP9-DL1-B1 (DL1) is the negative control. n=4, *p<0.05, **p<0.01, ****p<0.0001. (C) Fold-change in the relative mRNA expression of *IL1* and *TNF* receptor genes (*IL1R1, IL1Rap, IL1R2, TNFR1, TNFR2*) in E10.5 HBA endothelial cells (EC) and hematopoietic cells (HC) as compared to mesenchymal/other cells (MC). *IL1R1, IL1Rap, IL1R2, TNFR2* n=3 and *TNFR1* n=4, *p<0.05.

Figure 7. Pro-inflammatory factors are involved in HBA hematopoietic cell output. (A) Concentration (fg/ml) of TNFα protein in the supernatant of OP9-DL1-B1 cultures containing E10.5 (34-39 sp) HBA EC, MΦ or MIX (EC+MΦ), as determined by FCAP assay. n=3, *p=0.039, **p=0.005. Number of (B) CD45⁺ cells and (C) CFU-C number per one embryo equivalent (ee) of HBA cells in EC cultures supplemented with different TNFα concentrations. n=4, Number of (D) CD45⁺ cells and (E) CFU-C/ee of E10.5 HBA cells in the OP9-DL1-B1 cocultures containing EC, EC+TNFα nAb (neutralizing antibody 0.4µg/ml), EC+TNFα (10 ng/ml), MIX, MIX+TNFα neutralizing Ab (0.4µg/ml). n=4. Colony types are indicated by color bars. *p<0.05, **p<0.01, ***p<0.001.

Figure 1

A

B

0.7±0.05 — GFP vs FSC

99.6±0 — CD45 vs FSC

96.9±2.7 — CD11b vs F4/80

0.0 — GFP vs Gr1

C

% GFP$^+$ cells vs Embryonic day (9.5, 10.5, 11.5)

*** , *

D

CA, NE, V

i — CA

ii — NE, V

GFP
CD31

10 µm

E

Cx3cr1	Cxcr4	Ccr3
94.7	87.1	67.8

Ccr5	Ccr7	Cxcr2
18.8	0.1	0.1

# of Cells vs MFI

F

% in GFP$^+$ fraction vs Cx3cr1, Cxcr4, Ccr3, Ccr5, Ccr7, Cxcr2
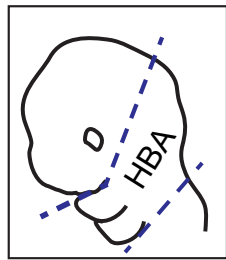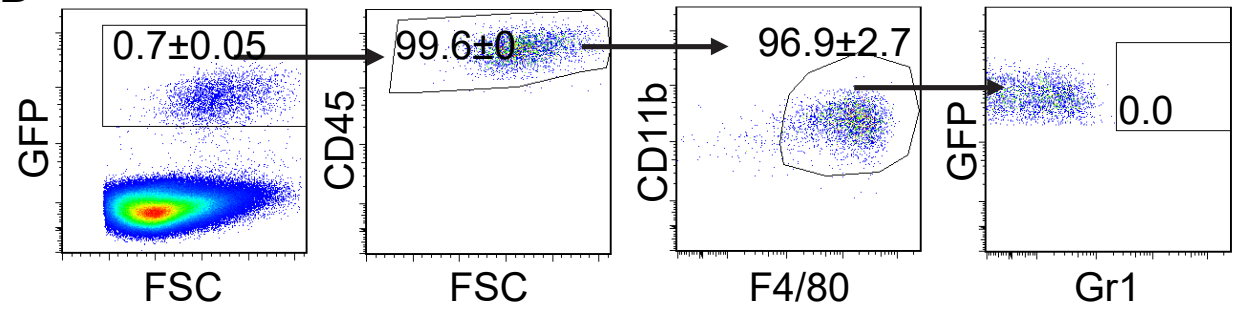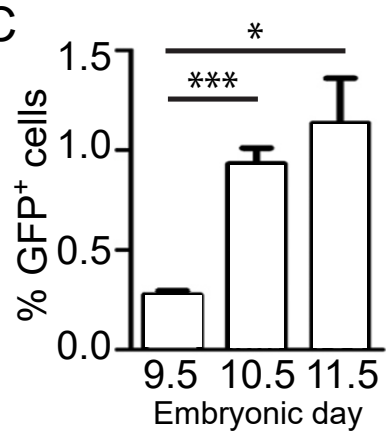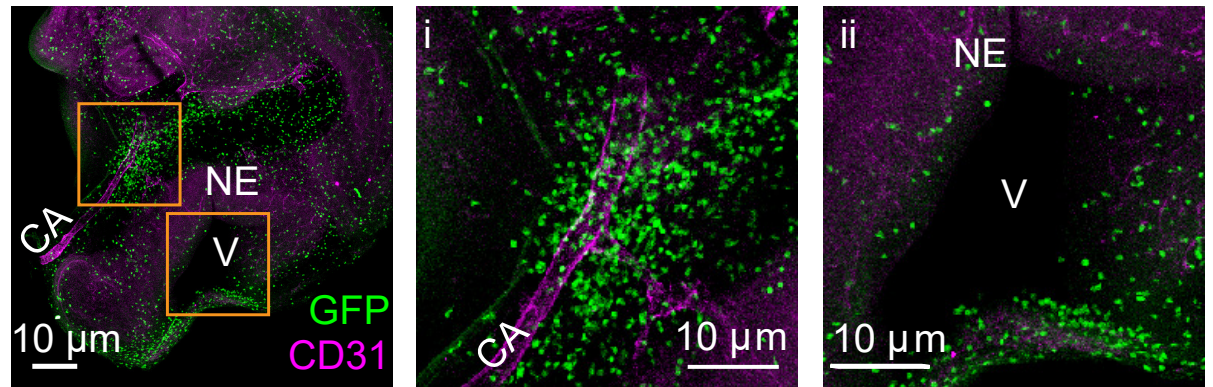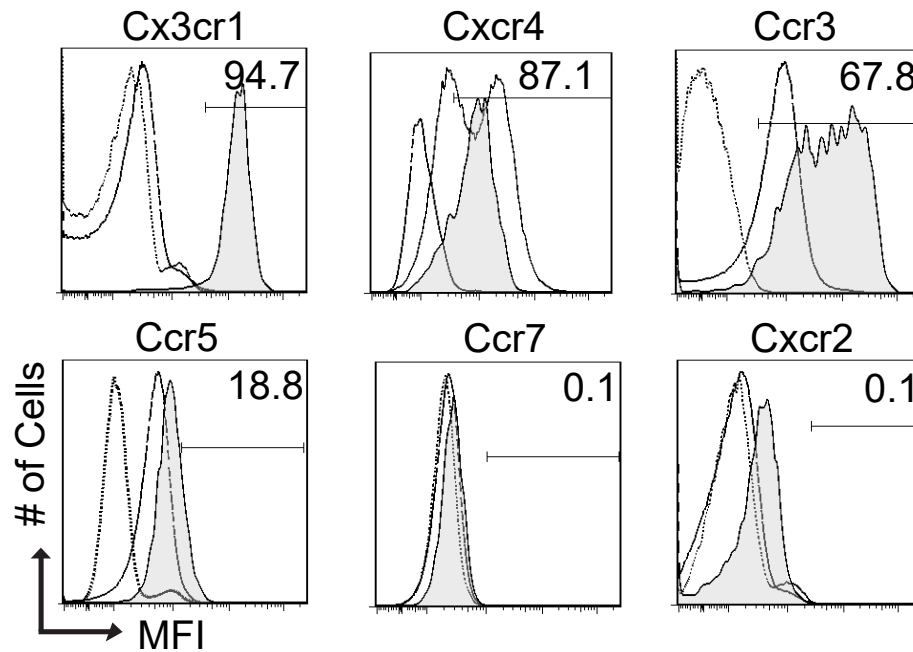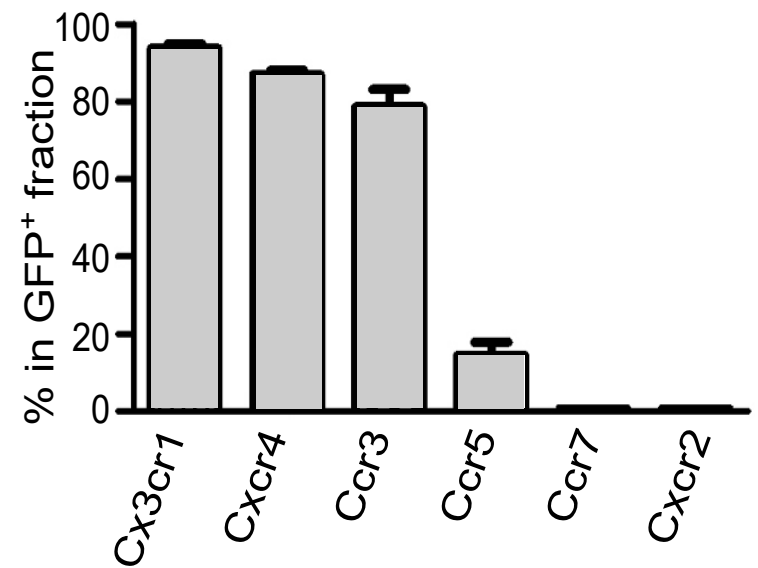
Figure 2

A
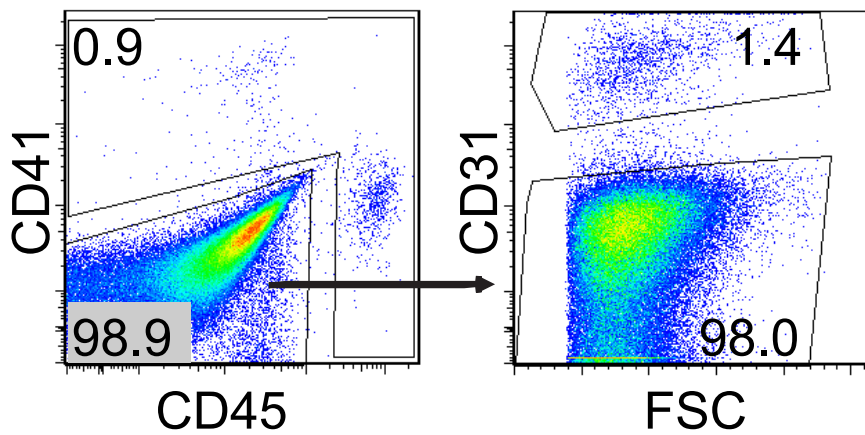
MC: CD31⁻CD41⁻CD45⁻
EC: CD31⁺CD41⁻CD45⁻
HC: CD41⁺ and/or CD45⁺

B

Figure 3

Figure 4

A. Schematic: *Cre* EC +/- WT Mφ → OP9-DL1-B1 → +/- BLZ945 7 days → CD45⁺ OP9-DL1-B1 → FACS → CD45⁺ → Methycellulose → CFU-C counts and genotype

B. EC, Mø, MIX micrographs (scale bar 50 μm)

C. CD45⁺ ($\times 10^3$)/ee — EC, Mø, MIX

D. CFU-C / ee — EC, Mø, MIX

E. CD45⁺ ($\times 10^4$)/ ee — EC^S, EC+BLZ, MIX^S, Mix+BLZ

F. CFU-C / ee — EC^S, EC+BLZ, MIX^S, Mix+BLZ

Legend:
- CFU-GEMM
- CFU-GM
- CFU-M
- CFU-G
- BFU-E
- CFU-E

Figure 5

Figure 6

A

B

C
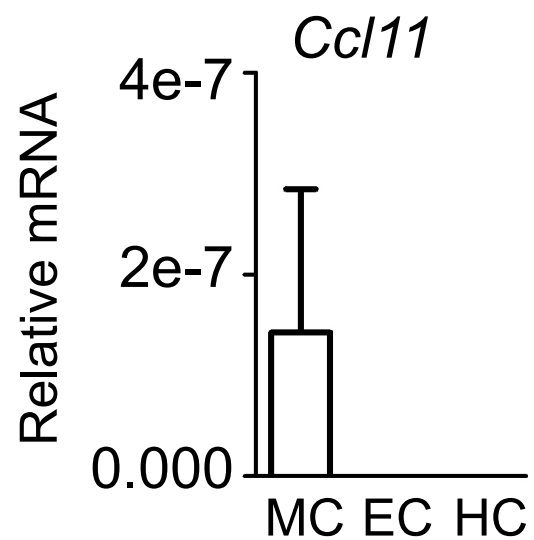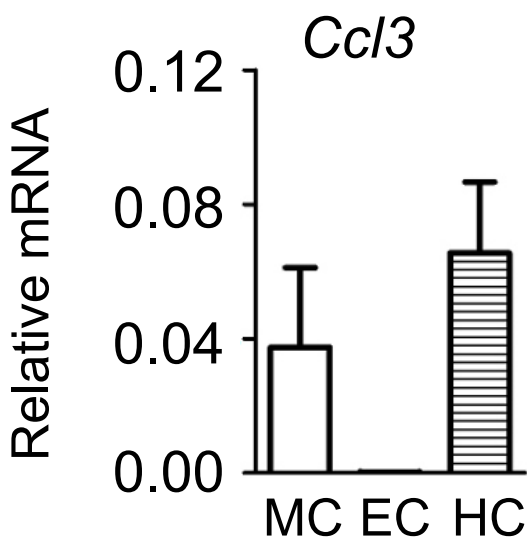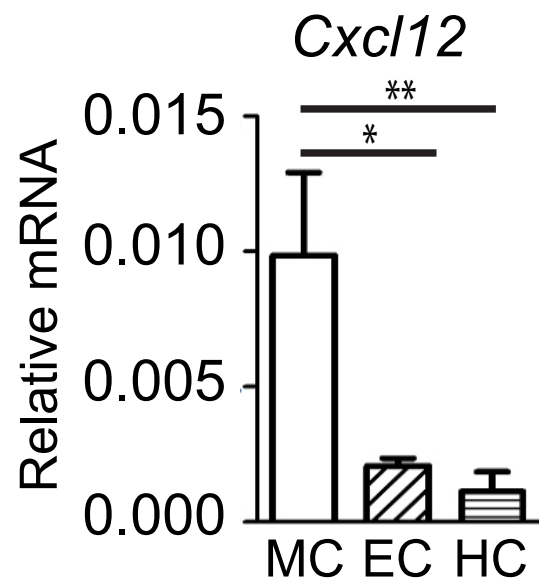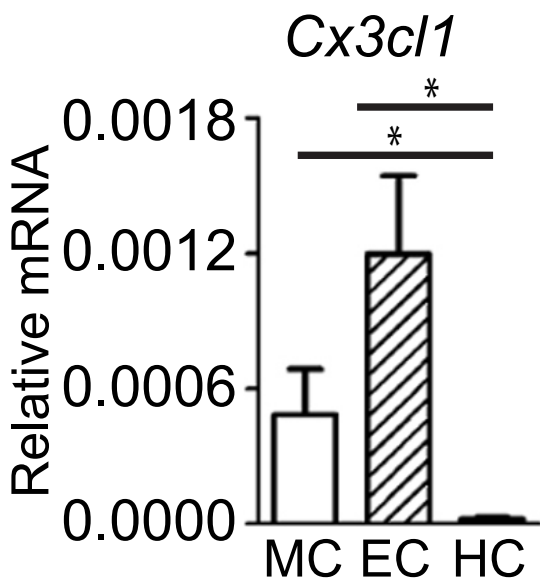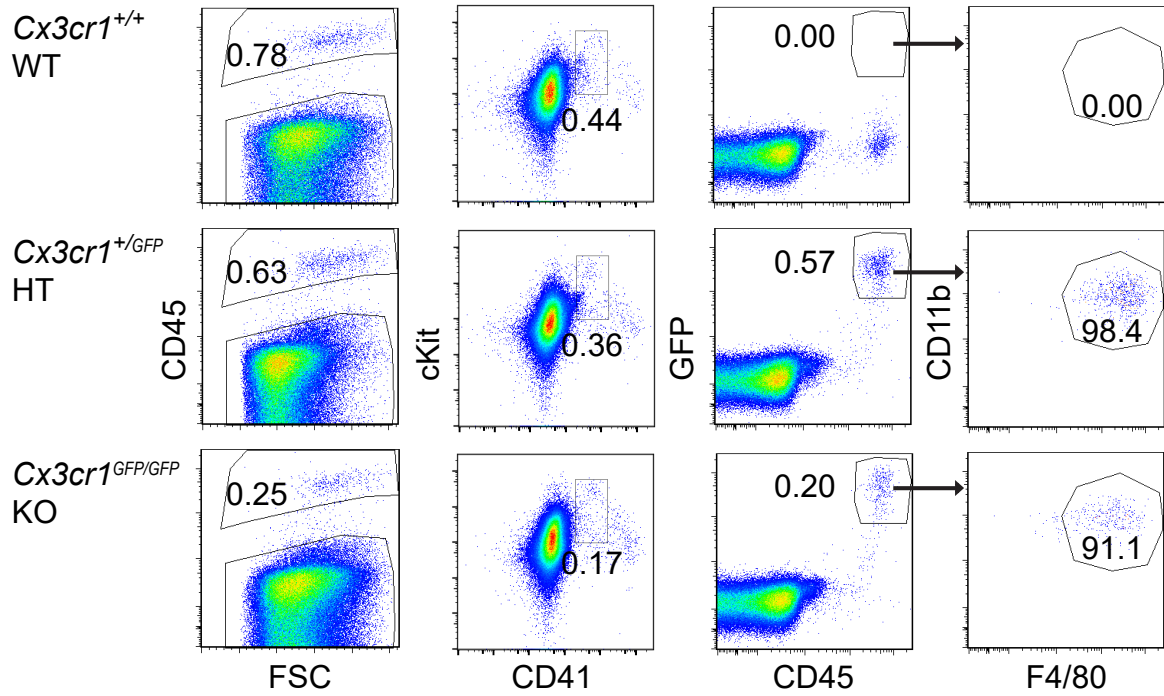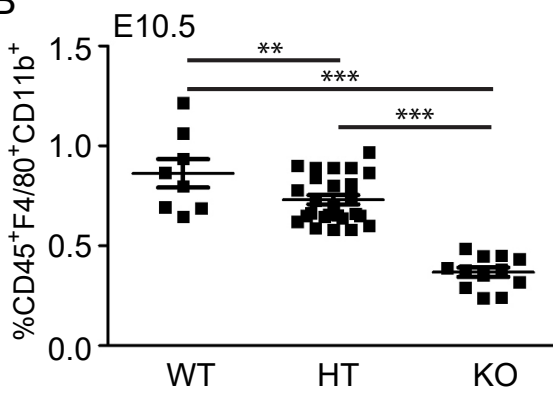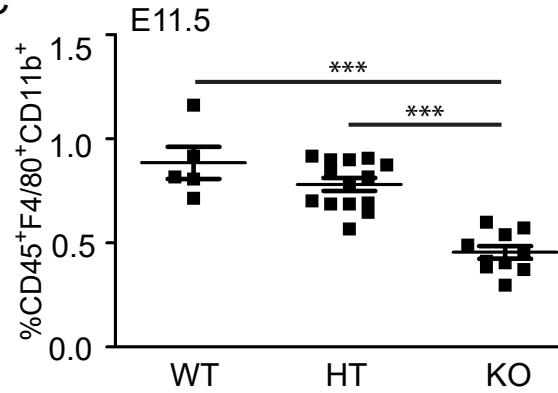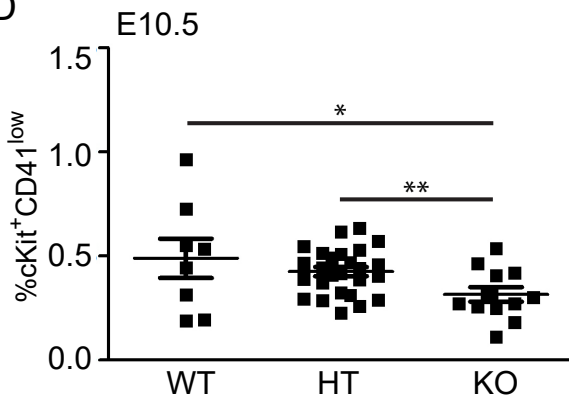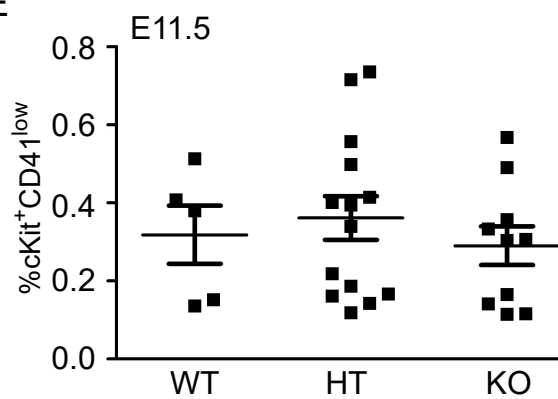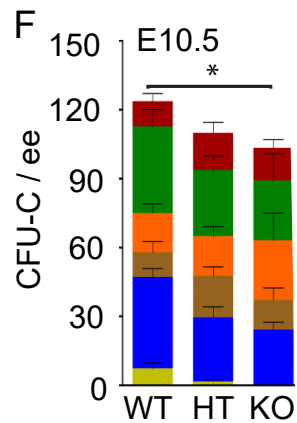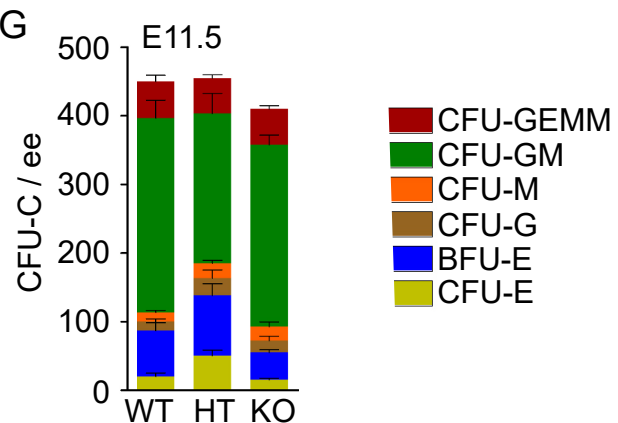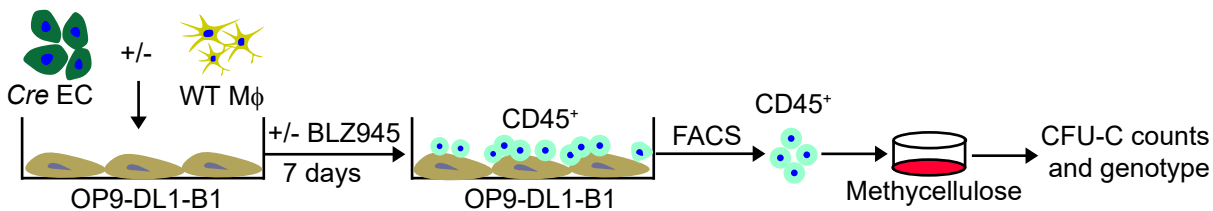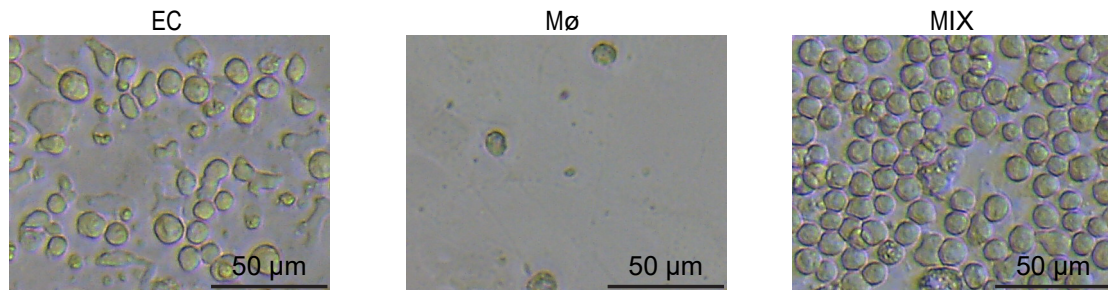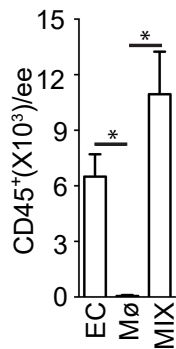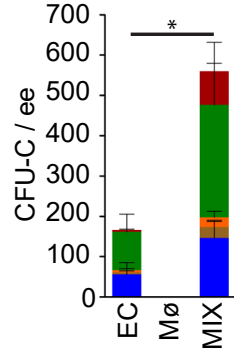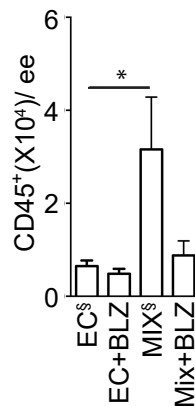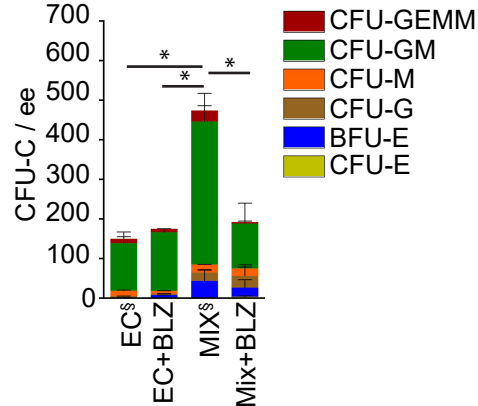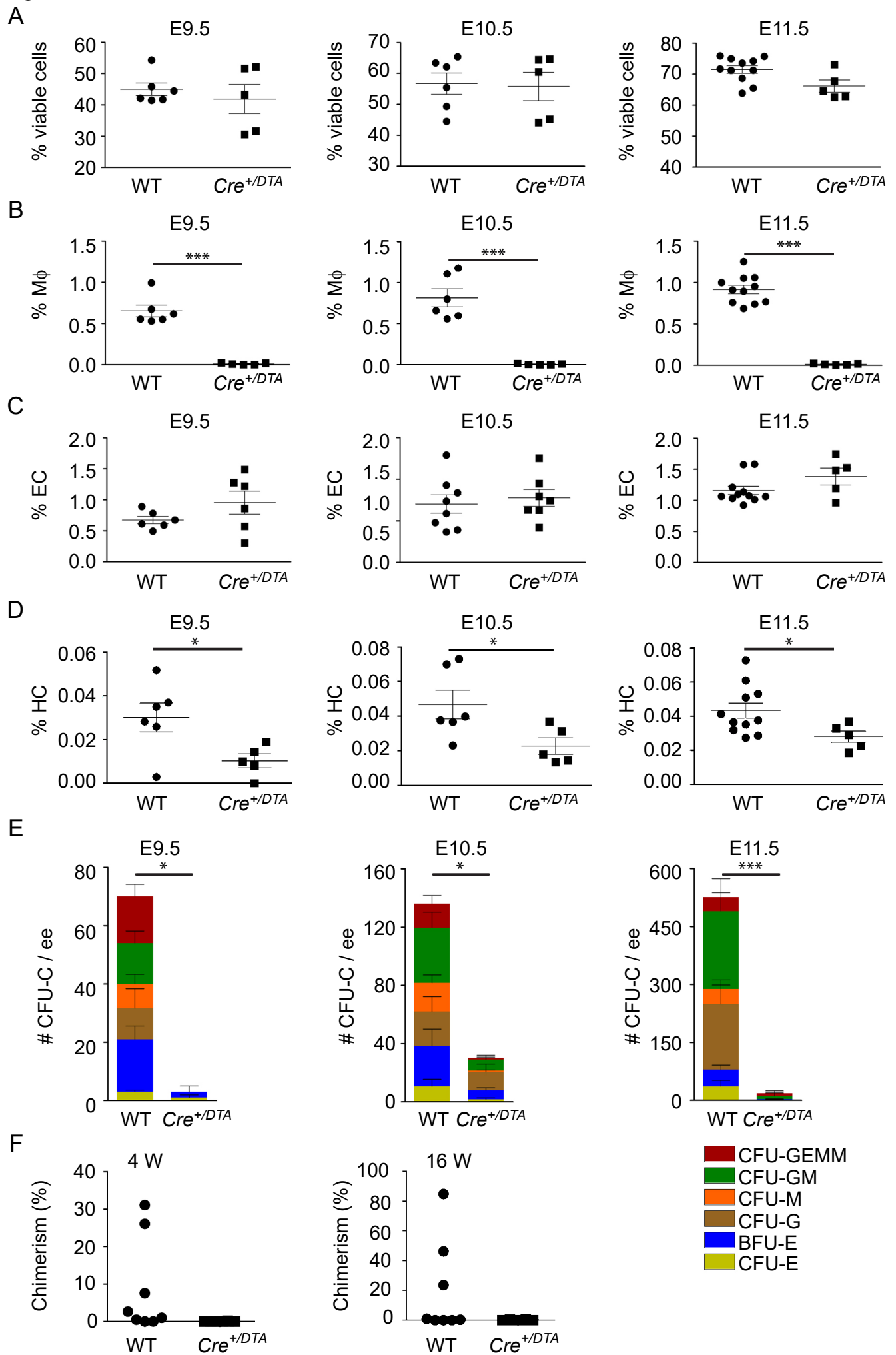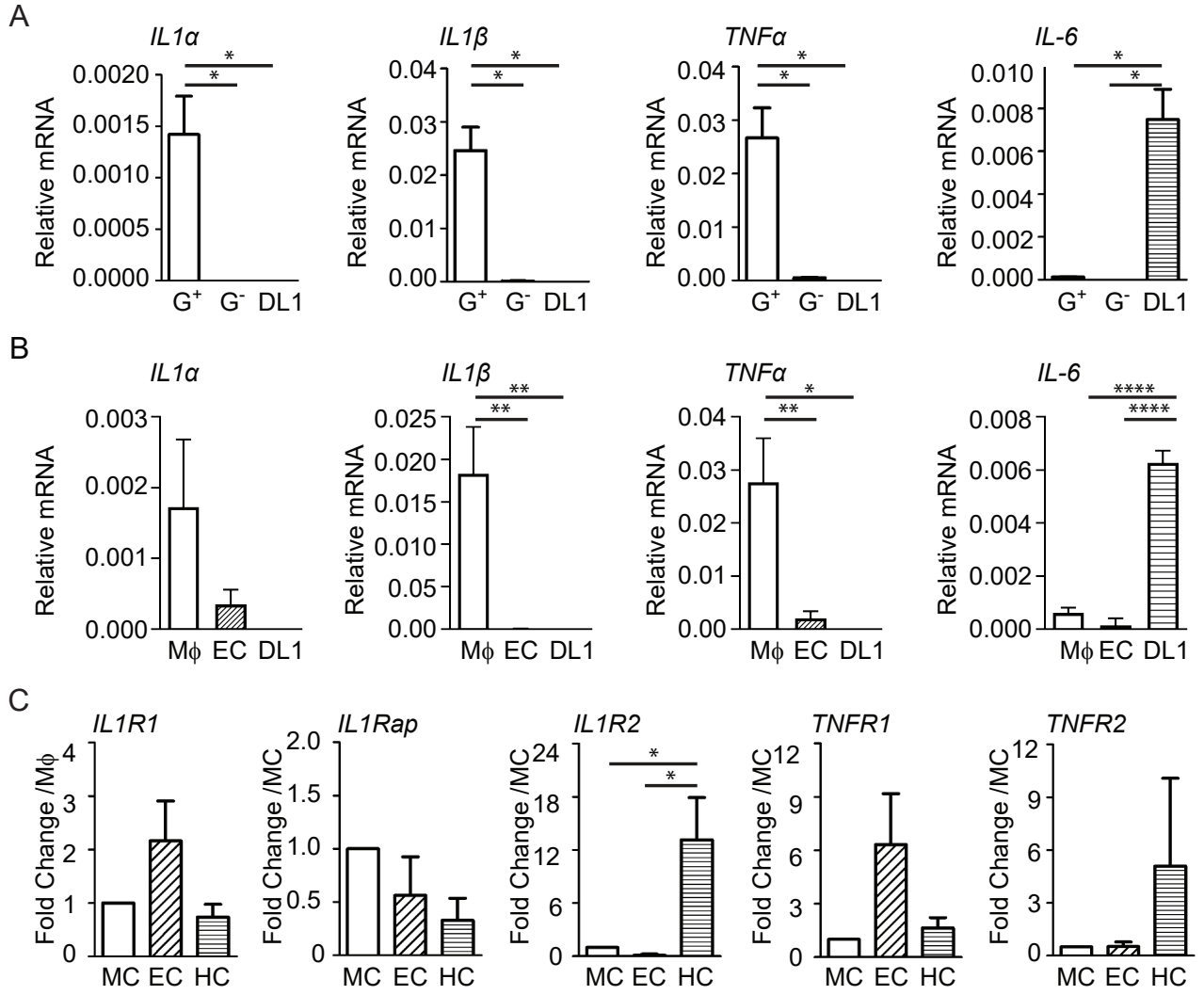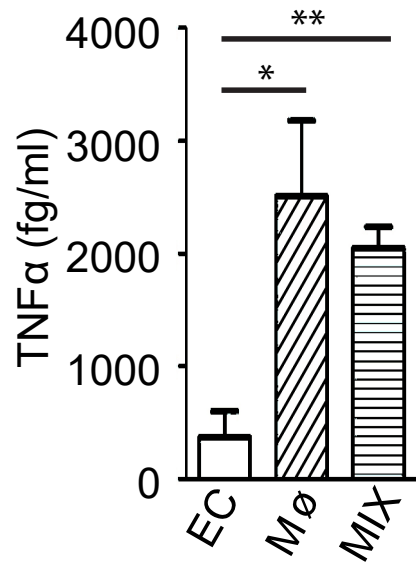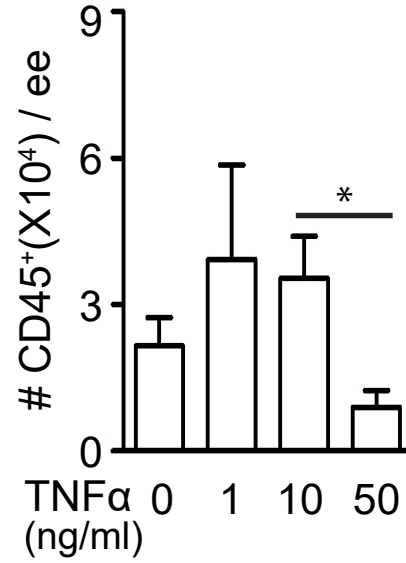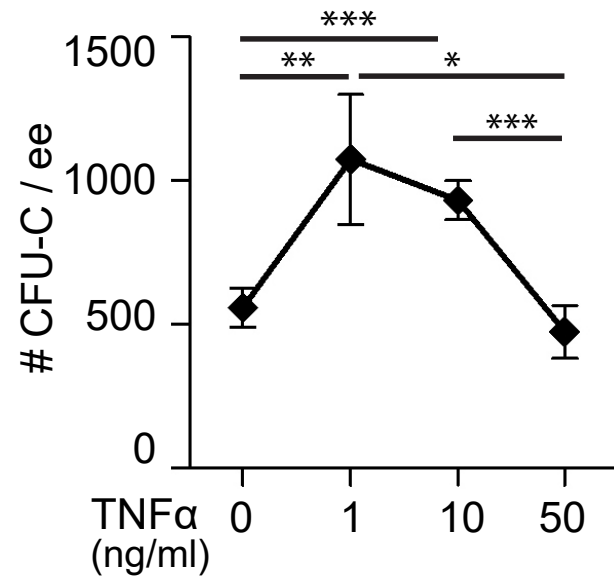
Figure 7

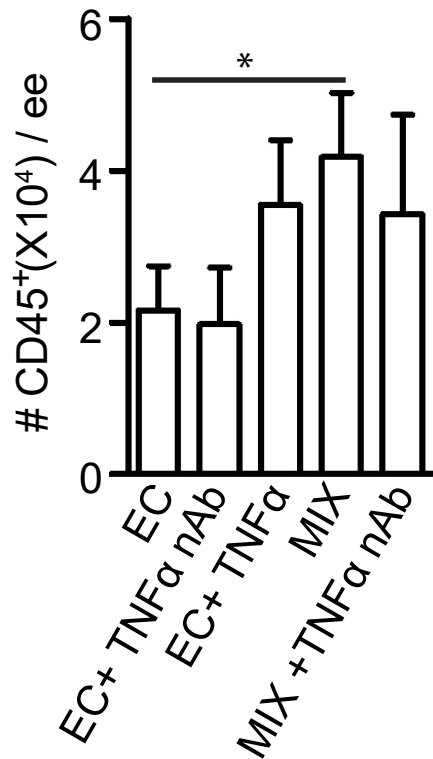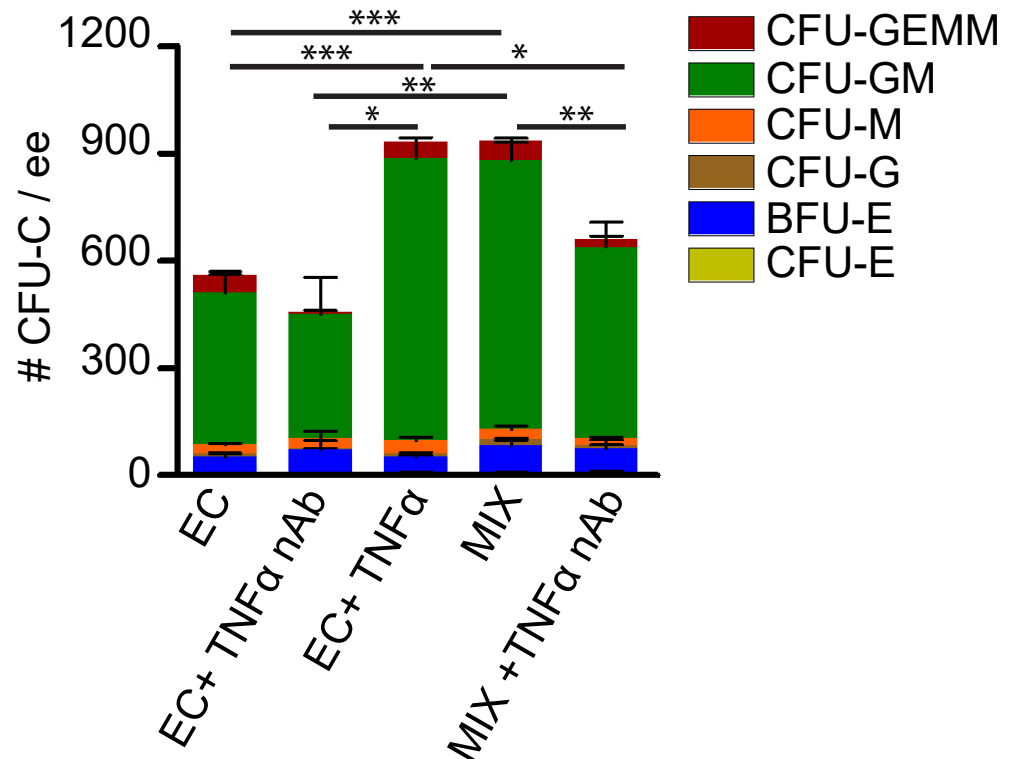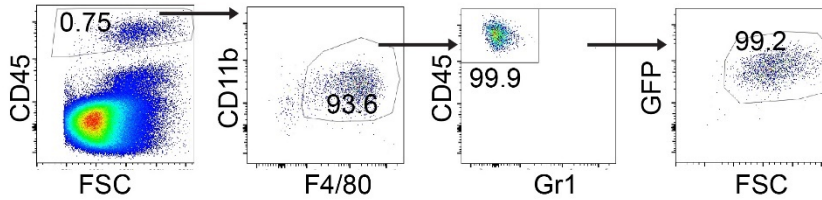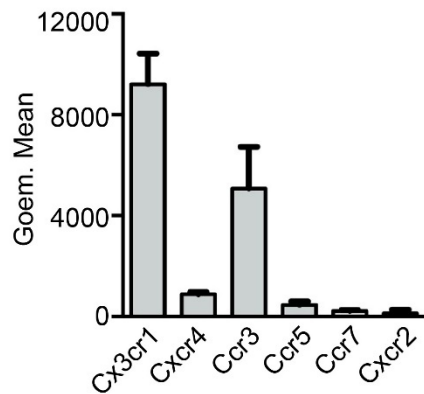**Supplemental Figures and Legends**

Sup Figure 1 (related to Fig 1)

A

B

**Supplemental Figure 1. Characterization of macrophages in E10.5 *MacGreen* HBA.** (A) Flow cytometric profiles for E10.5 *MacGreen* HBA cells showing that all CD45⁺CD11b⁺F4/80⁺Gr1⁻ macrophages cells are GFP⁺. Percentages shown in gated areas. FSC=forward scatter. (B) The Geometric Mean Fluorescence of chemokine receptors in the GFP⁺ fractions of E10.5 (32-39 sp) *MacGreen* HBA. n=4 for Cx3cr1, Ccr3, Ccr5, Ccr7 and n=3 for Cxcr4 and Cxcr2. Related to Figure 1.

Sup Figure 2 (related to Fig 3)

A

B
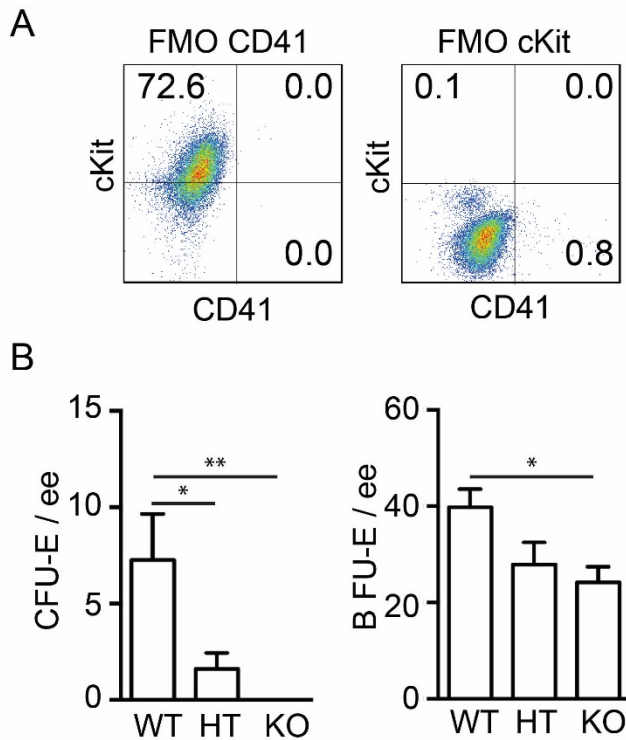
Supplemental Figure 2. Fluorescence minus one (FMO) controls and erthroid progenitor quantitation for the midgestation HBA. (A) Flow cytometric profiles showing gating for cKit and CD41 expressing cells. (B) CFU-E and BFU-E numbers per one embryo equivalent (ee) E10.5 HBA cells isolated from WT (wild type; *Cx3cr1*$^{+/+}$), HT (heterozygous; *Cx3cr1*$^{+/GFP}$) and KO (knockout; *Cx3cr1*$^{GFP/GFP}$) embryos. CFU-E=colony forming unit-erythroid; BFU-E=burst forming unit-erythroid. n=3, *p=0.05, p**=0.01. Related to Figure 3.
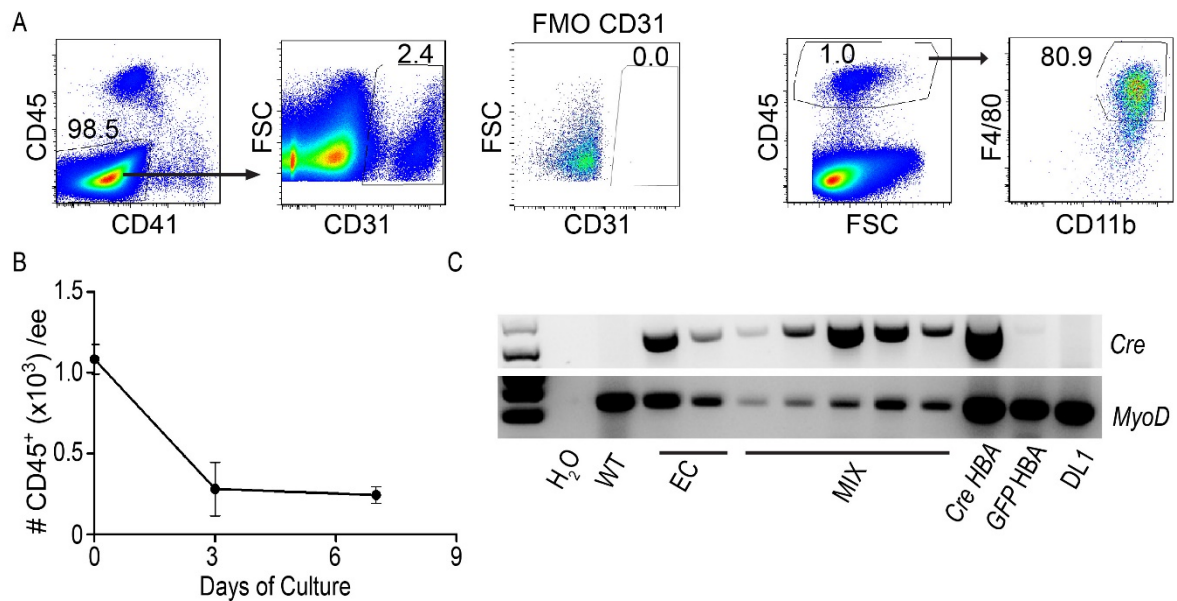
Supplemental Figure 3. Macrophages are involved in HBA hematopoietic cell formation *in vitro*. (A) Representative FACS data shows gating strategy of sorted endothelial cells (EC; CD41$^-$CD45$^-$CD31$^+$) and macrophages (Mφ; CD45$^+$F4/80$^+$CD11b$^+$) from E10.5 HBA. FMO CD31 as control for gating CD31. (B) Number of CD45$^+$ cells per embryo equivalent (ee) of HBA during culture. n=3. (C) Representative PCR genotyping data from individually harvested CFU-C following OP9-DL1-B1 culture. Endothelial cells used for culture carry the *Cre* transgene. Macrophages are transgene negative (WT; wild type). All CFU-Cs obtained from EC alone or EC+ Mφ (MIX) cultures are derived from endothelial cells. *Cre HBA*=positive control, *GFP HBA*=negative control, DL1=OP9-DL1-B1(*Bmp4* deletion). Related to Figure 4.
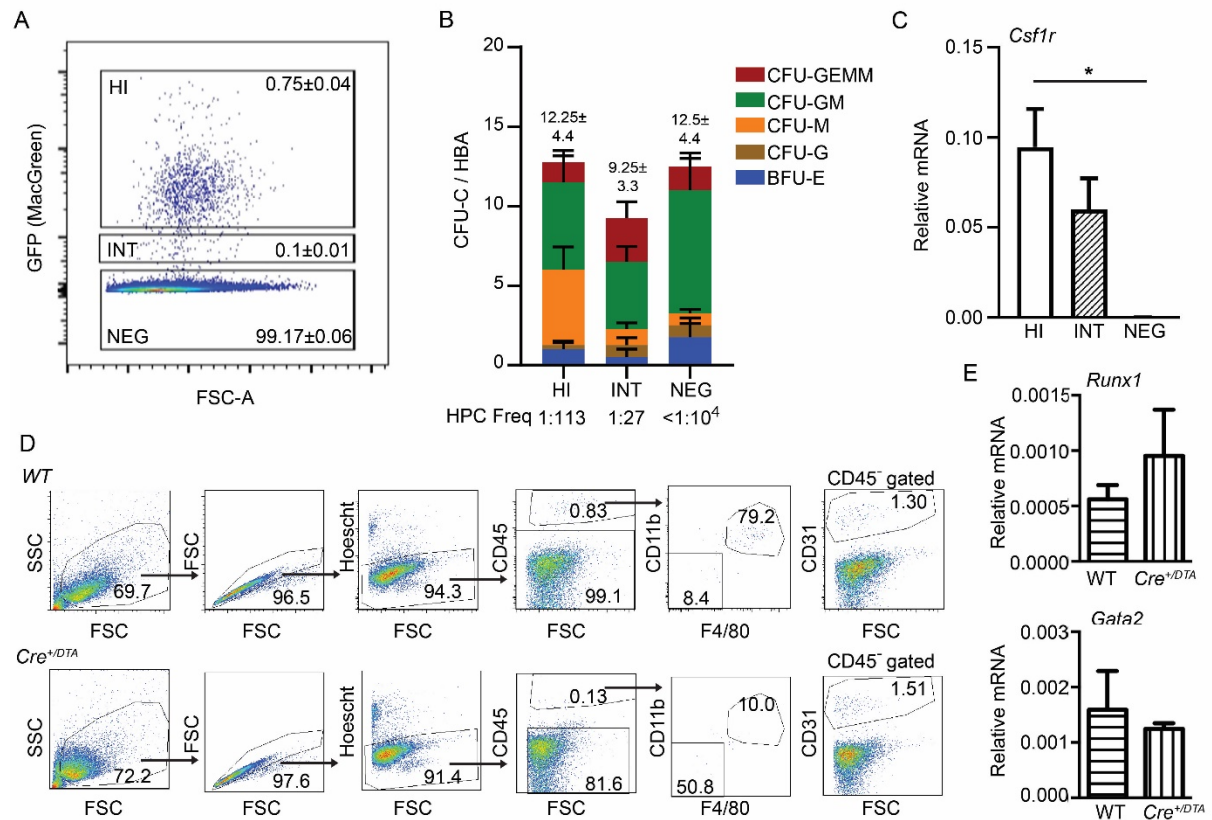
Supplemental Figure 4. HBA macrophages and some progenitors are *MacGreen* expressing and are reduced in the E10.5 *Csf1r^{Cre/DTA}* HBA. (A) Flow cytometric profile showing gates for GFP HI- (high), INT- (intermediate), and NEG-(negative) expressing HBA cells from E10.5 *MacGreen* embryos. (B) CFU-C number per one embryo equivalent of GFP^{HI}, GFP^{INT} and GFP^{NEG} sorted E10.5 HBA cells from E10.5 *MacGreen* embryos. Number of individual colony types are indicated. CFU-C=colony forming unit-cell; GEMM= granulocyte, erythroid, macrophage, megakaryocyte; GM=granulocyte, macrophage; M=macrophage; G=granulocyte; E=erythroid. (C) Relative mRNA expression of *Csf1r* in GFP^{HI}, GFP^{INT} and GFP^{NEG} sorted E10.5 HBA cells from E10.5 *MacGreen* embryos as determined by qRT-PCR. *Actin* was used as the normalization control. SEM is shown. n=3, *p<0.05. (D) Representative flow cytometric data showing gating strategy of E10.5 *WT* (wild type) and *Csf1r-Cre^{+/DTA}* HBA cells. (E) Relative mRNA expression of R*unx1* and G*ata2* in endothelial cells of *WT* (wild type) and *Csf1r-Cre^{+/DTA}* E10.5 HBA as determined by qRT-PCR. *Actin* was used as the normalization control. Related to Figure 5.

Supplemental Tables

Supplemental Table 1. PCR primer sequences for genotyping

Cx3cr1 Wild type-Forward	5'-GTCTTCACGTTCGGTCTGGT-3'
Cx3cr1 Mutant-Forward	5'-CTCCCCCTGAACCTGAAAC-3'
Cx3cr1 Common-Reverse	5'-CCCAGACACTCGTTGTCCTT-3'
Cxr1r-Cre-Forward	5'-CTGGCTGTGAAGACCATC-3'
Csf1r-Cre-Reverse	5'-CAGGGCCTTCTCCACACCAGC-3'
RosaDTA-Forward	5'-GACGCTGCGGGATACTCTGT-3'
RosaDTA-Reverse	5'-CTGAGCACTACACGCGAAGC-3'

Supplemental Table 2. Antibody list

Antibody	Clone No.	company
CD31 AF647	MEC13.3	BD Bioscience
CD45 PE	30-F11	BD Bioscience
CD41 eFluor450	MWReg30	eBioscience
CD11b BV605	M1/70	eBioscience
F4/80 PECy5	BM8	eBioscience
Cx3cr1 BV650	SA011E11	Biolegend
Cxcr4 PE Dazzle594	L276F12	Biolegend
Ccr3 PECy7	J073E5	Biolegend
Ccr5 PE	HM-CCR5	Biolegend
Ccr7 BV421	4B12	Biolegend
Cxcr2 PerCP Cy5.5	SA045E1	Biolegend
CD45.1 APC	A20	BD Bioscience
CD45.2 PE	104	BD Bioscience
CD31 Biotin	MEC13.3	BD Bioscience
GFP	598	MBL

Supplemental Table 3. Primer sequences for qRT-PCR

IL1a-Forward	5'- CGAAGACTACAGTTCTGCCATT -3'
IL1a-Reverse	5'- GACGTTTCAGAGGTTCTCAGAG -3'
IL1β-Forward	5'- TGGACCTTCCAGGATGAGGACA -3'
IL1β- Reverse	5'- GTTCATCTCGGAGCCTGTAGTG -3'
TNFa -Forward	5'- GGTGCCTATGTCTCAGCCTCTT -3'
TNFa - Reverse	5'- GCCATAGAACTGATGAGAGGGAG -3'
IL6 -Forward	5'- TAGTCCTTCCTACCCCAATTTCC -3'
IL6 - Reverse	5'- TTGGTCCTTAGCCACTCCTTC -3'
IL1R1-Forward	5'- CACTGGACCTCGGGTAACTC -3'
IL1R1- Reverse	5'- TTGGTCCTTAGCCACTCCTTC -3'
IL1Rap -Forward	5'- TGCCTGGGGGAATTGTCAC -3'
IL1Rap - Reverse	5'- CTTAGCCCGCTTCAGCTCTTT -3'
IL1R2-Forward	5'- GTTTCTGCTTTCACCACTCCA -3'
IL1R2- Reverse	5'- GAGTCCAATTTACTCCAGGTCAG -3'
Tnfrsf1a- Forward	5'- CCGGGAGAAGAGGGATAGCTT -3'
Tnfrsf1a- Reverse	5'- TCGGACAGTCACTCACCAAGT -3'
Tnfrsf1b- Forward	5'- ACACCCTACAAACCGGAACC -3'
Tnfrsf1b- Reverse	5'- AGCCTTCCTGTCATAGTATTCCT -3'
Cx3cl1-Forward	5'- CCCAGACAGAAGTCATAGCCA -3'
Cx3cl1- Reverse	5'- ACACATCCAGACACCGTTGG -3'
Cxcl12-Forward	5'- AGAGCCCTAGACCCATTTCCT -3'
Cxcl12- Reverse	5'- CATTCTTCAGGGTGGCTATGA -3'
Ccl3-Forward	5'- TTCTCTGTACCATGACACTCTGC -3'
Ccl3- Reverse	5'- CGTGGAATCTTCCGGCTGTAG -3'
Ccl7-Forward	5'- GCTGCTTTCAGCATCCAAGTG -3'
Ccl7- Reverse	5'- CCAGGGACACCGACTACTG -3'
β Actin- Forward	5'- CACCACACCTTCTACAATGAG -3'
β Actin- Reverse	5'- GACCCAGATCATGTTTGAGAC -3'

Supplemental Table 4. Cell number in WT, Cx3cr$^{GFP/+}$ (HT), Cx3cr1$^{GFP/GFP}$ (KO) HBAs

Embryo stage	Genotype	Cell Number (mean±SEM, X10^5)	Number of experiments
E10.5	WT	4.02±0.27	3
	HT	4.78±0.08	3
	KO	4.11±0.14	4
E11.5	WT	13.45±0.81	3
	HT	13.35±0.65	3
	KO	14.90±0.7	3

Supplemental Table 5. Numbers of WT and *Csf1r-Cre*[+/DTA] embryos

Embryo stage	Genotype	Number of embryos	Number of experiments	*Csf1r-Cre*[+/DTA] embryos: total embryos
E10.5	WT	39	7	12:51=0.24
	Csf1r-Cre[+/DTA]	12		
E11.5	WT	88	9	34:122=0.28
	Csf1r-Cre[+/DTA]	34		

Supplemental Table 6. Numbers of cells obtained from WT and *Csf1r-Cre*[+/DTA] HBAs

Embryo stage	Genotype	Cell Number (mean±sem, x10^5)	Number of experiments
E9.5	WT	1.2±0.13	6
	Csf1r-Cre[+/DTA]	1.0±0.07	5
E10.5	WT	5.0±0.67	4
	Csf1r-Cre[+/DTA]	4.98±0.51	4
E11.5	WT	13.23±2.30	4
	Csf1r-Cre[+/DTA]	11.48±1.15	5